JPET Fast Forward. Published on July 26, 2005 as DOI: 10.1124/jpet.105.090886


JPET# 90886

# Analysis of Allosterism in Functional Assays [a]

Frederick J. Ehlert

Department of Pharmacology

College of Medicine

University of California, Irvine

Irvine, California 92697-4625

JPET Fast Forward. Published on July 26, 2005 as DOI: 10.1124/jpet.105.090886
This article has not been copyedited and formatted. The final version may differ from this version.



Running title: Analysis of allosterism

To whom correspondence should be addressed:

Frederick J. Ehlert, Ph.D.

Department of Pharmacology

University of California, Irvine

Irvine, California 92697-4625

Tel: 949-824-3709

FAX: 949-824-4855

e-mail: fjehlert@uci.edu

Number of text pages: 27

Number of tables: 5

Number of figures: 9

Number of references: 22

Number of words in *Abstract*: 232

Number of words in *Introduction*: 641

Number of words in *Discussion*: 1412

Abbreviations: $\alpha$, cooperative effect of the allosteric modulator on agonist affinity; ß, cooperative effect of the allosteric modulator on agonist efficacy; BM-5, N-(4-pyrrolidino-2-butynyl)-N-methylacetamide; $EC_{50}$, concentration of agonist eliciting half-maximal response; $E_{max}$, maximal response; $\gamma$, ratio of ß/$\alpha$; $K_A$, dissociation constant of allosteric modulator; $K_X$, dissociation constant of agonist; *RA*, relative activity of the agonist in the presence of the allosteric modulator.

Section assignment: Cellular and Molecular

JPET Fast Forward. Published on July 26, 2005 as DOI: 10.1124/jpet.105.090886
This article has not been copyedited and formatted. The final version may differ from this version.



## ABSTRACT

The theoretical basis for analyzing the effects of an allosteric modulator on the response to an agonist is described. The effects of an allosteric modulator on the concentration-response curve to an agonist can be attributed to changes in the observed dissociation constant and intrinsic efficacy of the agonist-receptor complex. Each of these two changes can be represented by a coefficient or factor. It is possible to estimate the ratio of the coefficient of change in agonist efficacy divided by that for the agonist dissociation constant. This ratio is designated as the relative activity of the agonist in the presence of the allosteric modulator (*RA*). The *RA* value can be estimated for each concentration of allosteric modulator by nonlinear regression analysis, regardless of the shape of the concentration-response curve. Regression analysis of the *RA* values against the concentration of allosteric modulator yields estimates of the dissociation constant ($K_A$) of the allosteric modulator and the maximal *RA* value. If the concentration-response curve to the agonist obeys a logistic function and the allosteric modulator influences the maximal response, it is possible to distinguish between the maximal change in affinity from that of efficacy. If the agonist concentration-response curve obeys a logistic equation with a Hill slope of one, the *RA* values can be estimated easily from the agonist $EC_{50}$ and $E_{max}$ values. This analysis illustrates the utility of the *RA* value in quantifying allosteric effects.

JPET Fast Forward. Published on July 26, 2005 as DOI: 10.1124/jpet.105.090886
This article has not been copyedited and formatted. The final version may differ from this version.



# INTRODUCTION

Drugs that act allosterically to modify receptor function have unique advantages over those that bind directly to the primary recognition site of a receptor. The latter agents produce a continuous effect, whereas allosteric drugs only tune up or tune down signaling when the endogenous neurotransmitter is released (Burgen, 1981; Ehlert, 1986; Christopoulos, 2002). Thus, allosteric drugs preserve the temporal pattern of signaling across the synapse or neuroeffector junction. Also, with overdose, high concentrations of a directly acting agonist or antagonist can cause excessive receptor activation or inhibition, whereas the maximal effect of an allosteric drug has a ceiling depending upon the nature of its allosteric effect. Thus, protection against overdose can be achieved with allosteric drugs.

There are three pharmacodynamic properties that determine the effects of an allosteric drug on the action of an agonist or endogenous neurotransmitter. These properties are 1) the affinity ($K_D$) of the allosteric drug for its site on the receptor, 2) its modulatory effect on the affinity of the agonist-receptor complex (cooperativity), and 3) its modulatory effect on the intrinsic efficacy of the agonist-receptor complex. Several investigators have described methods for measuring the affinities and cooperative effects of allosteric drugs in radioligand binding assays (Stockton et al., 1983; Ehlert, 1988a; Lazareno and Birdsall, 1995). However, to date, there have been few attempts to discriminate between allosteric effects on agonist affinity and intrinsic efficacy in functional assays. Moreover, it is often assumed that the methods presently available for investigating allosterism in functional assays are valid only if the allosteric agent is without effect on the intrinsic efficacy of the agonist-receptor complex. However, a null method (Ehlert, 1988a) was described quite some time ago for estimating allosteric ligand affinities in functional assays under conditions where the allosteric agent modulates either the affinity or intrinsic efficacy of the agonist or both. The method was based on the assumption that the intrinsic efficacy of the agonist-receptor-allosteric drug complex (*XRA*) could be different from that of the agonist-receptor complex (*XR*). By deriving the mathematical equation for the

combined stimulus elicited by both receptor complexes (i.e., *XR* and *XRA*), it was possible rearrange the latter equation to derive a null equation for comparing equivalent tissue responses in the presence and absence of an allosteric drug (Ehlert, 1988a). In the prior report, simple methods for applying the null equation to evaluate allosteric changes in agonist affinity and efficacy were described for highly efficacious agonists exhibiting a large receptor reserve or for situations with little receptor reserve only involving a change in affinity. In principle, it should be possible to apply these mathematics to all conditions using nonlinear regression analysis.

In the present report, the theory for investigating allosteric interactions in functional assays is described. This theory is applied to predict the behavior of the concentration-response curve of an agonist in the presence of allosteric drugs that modify agonist affinity and efficacy. Three mathematical methods are described and applied to analyze the theoretical data. These are 1) a null method, which requires no assumption regarding the nature of the stimulus-response relationship, 2) a method based on a logistic relationship between the stimulus and response (i.e., operational model), and 3) a special case of the former method, in which the Hill slope of the concentration-response curve equals one. Finally, methods based on the operational model are used to analyze experimental data from the literature. The results show that it is possible to estimate the affinity of an allosteric drug in functional assays regardless of whether it influences the affinity and intrinsic efficacy of the agonist. Under all conditions, it is possible to measure the product of the allosteric changes in efficacy and affinity (i.e., reciprocal of the dissociation constant). If the allosteric agent influences the maximal response of the agonist, it is possible to distinguish the allosteric change in affinity from the change in efficacy.

JPET Fast Forward. Published on July 26, 2005 as DOI: 10.1124/jpet.105.090886
This article has not been copyedited and formatted. The final version may differ from this version.



# METHODS

## Theory

*Allosterism*: An allosteric drug binds at a secondary allosteric site on the receptor, distinct from the site at which the agonist binds. The scheme showing the interaction of an allosteric drug (*A*) with an agonist (*X*) at a receptor (*R*) is:

$$\begin{array}{ccc} [X]+[R]+[A] & \xleftrightarrow{K_X} & [XR]+[A] \\ K_A \updownarrow & & \updownarrow \alpha K_A \\ [X]+[RA] & \xleftrightarrow{\alpha K_X} & [XRA] \end{array}$$

in which, $K_X$ denotes the dissociation constant of the agonist-receptor complex, $K_A$ denotes the dissociation constant of the allosteric drug-receptor complex, and $\alpha K_A$ and $\alpha K_X$ denote the corresponding dissociation constants when the receptor is occupied by both ligands. Receptor theory posits that the response to an agonist is a function (*f*) of the stimulus, with the stimulus being equivalent to the product of receptor occupancy and intrinsic efficacy (Stephenson, 1956; Furchgott, 1966). If it is assumed that the *RA* complex is inactive, then the stimulus (*S*) of an agonist in the presence of an allosteric drug is given by (Ehlert, 1988a):

$$S = \varepsilon[XR] + \varepsilon'[XRA] \qquad 1$$

in which $\varepsilon$ and $\varepsilon'$ denote the intrinsic efficacies of the *XR* and *XRA* complexes, respectively. As described previously (Ehlert, 1988a), making the appropriate substitutions yields:

$$S = \frac{\varepsilon XR_T}{X + K_X + AX/\alpha K_A + \alpha K_X/K_A} + \frac{\varepsilon' XR_T}{X + \alpha K_X + \alpha X K_A/A + \alpha K_A K_X/A} \qquad 2$$

in which $R_T$ denotes the total amount of receptors. This equation simplifies to:

$$S = \frac{Xq\varepsilon R_T}{X + pK_X} \qquad 3$$

in which

$$p = \frac{1 + A/K_A}{1 + A/\alpha K_A} \qquad 4$$

$$q = \frac{1 + \beta A/\alpha K_A}{1 + A/\alpha K_A} \qquad 5$$

JPET Fast Forward. Published on July 26, 2005 as DOI: 10.1124/jpet.105.090886
This article has not been copyedited and formatted. The final version may differ from this version.



$$ß = \frac{\varepsilon'}{\varepsilon} \qquad 6$$

An equivalent form of equation 3 has been described by Christopoulos (see equation 1.21.8 (Christopoulos, 2000)). Also, the activation state model of Hall (2000) for allosteric interactions is entirely consistent with equation 3 under the condition where little receptor is active in the absence of agonist and the *RA* complex is inactive. Equation 3 shows that, in the absence of the allosteric modulator (i.e., $A = 0$ and therefore $p = 1$ and $q = 1$), the stimulus function resembles a one-site model with a maximum proportional to $\varepsilon R_T$ and the concentration of agonist eliciting a half-maximal stimulus equivalent to $K_X$. The effect of the allosteric modulator is to cause a concentration-dependent modification in either the observed dissociation constant or the maximal stimulus or both by the coefficients *p* and *q*, respectively. If it were possible to measure the stimulus directly - such as in voltage clamp experiments on a ligand-gated ion channel with a simple one-site occupancy curve - one could use regression analysis to fit equations 4 and 5 to the estimates of the relative change in potency and maximal current, respectively, to obtain estimates of $K_X$, $\alpha$ and ß. Similarly, in enzyme assays, where the activity of the enzyme is measured directly, one could use regression analysis to fit equations 4 and 5 to the estimates of the allosteric change in the maximum velocity ($V_{max}$) and Michaelis constant ($K_m$) to obtain the allosteric parameters $K_X$, $\alpha$ and ß. However in most pharmacological assays of function, it is impossible to measure the stimulus directly. Rather, a consequent, downstream response is usually measured. In this situation, the response can be described by the following equation:

$$response = f\left(\frac{Xq\varepsilon R_T}{X + pK_X}\right) \qquad 7$$

in which *f* denotes the unknown stimulus-response function. Below, three different approaches for estimating the influence of an allosteric modulator on the affinity and efficacy of the agonist-receptor complex are described. The first involves eliminating the stimulus-response function from the analysis through the use of a null method. The second involves the use of the operational model to describe the stimulus-response function, and the third involves a special

case of the operational model in which the Hill slope of the concentration-response curve equals one.

*Null method*: One approach to estimate allosteric effects in functional assays is to compare equivalent tissue responses in the presence and absence of the allosteric drug (see Ehlert (1988a)) so that the unknown relationship between the stimulus and response is eliminated. Using this approach, the relationship describing equivalent tissue responses in the absence and presence of an allosteric drug is given by:

$$f\left(\frac{\varepsilon X R_T}{X + K_X}\right) = f\left(\frac{X' q \varepsilon R_T}{X' + pK_X}\right) \qquad 8$$

in which $X$ and $X'$ denote the equiactive concentrations of agonist in the absence and presence of the allosteric drug, respectively. This equation simplifies to:

$$X = \frac{qX'K_X}{X'(1-q) + pK_X} \qquad 9$$

Equation 9 can also be rearranged in the form:

$$X' = \frac{pK_X}{q(1 + K_X/X) - 1} \qquad 10$$

It is useful to define the term relative activity of the agonist in the presence of the allosteric modulator (*RA*), which represents the ratio of the allosteric change in intrinsic efficacy ($q$) divided by the allosteric change in the dissociation constant of the agonist ($p$):

$$RA = \frac{q}{p} \qquad 11$$

Making the appropriate substitutions for $p$ (equation 4) and $q$ (equation 5) yields:

$$RA = \frac{1 + \gamma A/K_A}{1 + A/K_A} \qquad 12$$

in which:

$$\gamma = \frac{\beta}{\alpha} \qquad 13$$

The method for using equations 9, 10, 11 and 12 for the analysis of allosteric effects in functional assays is described below under "Results."

JPET Fast Forward. Published on July 26, 2005 as DOI: 10.1124/jpet.105.090886
This article has not been copyedited and formatted. The final version may differ from this version.



*Operational model*: Although the null method just described has the advantage of being applicable for any type of stimulus-response function (i.e., any shape of concentration response curve), it is widely observed that agonists usually exhibit logistic concentration-response curves. Indeed a curve fitting procedure based on the following logistic equation is the most common computational method that investigators use to estimate the maximal response ($E_{max}$) and concentration of agonist eliciting half-maximal response ($EC_{50}$):

$$response = \frac{X^n E_{\max}}{X^n + EC_{50}{}^n} \qquad 14$$

in which $n$ denotes the Hill slope. Several investigators have shown that if the input to the stimulus-response function ($f$) is the stimulus (i.e., product of receptor occupancy and intrinsic efficacy) and the output obeys the logistic function just described, then the stimulus-response function must be the following (Furchgott, 1966; Mackay, 1981; Kenakin and Beek, 1982; Black and Leff, 1983):

$$response = \frac{S^m M_{sys}}{S^m + K_E{}^m} \qquad 15$$

in which $M_{sys}$ denotes the maximum response of the system, $K_E$ denotes the sensitivity of the stimulus-response function and $m$ denotes the transducer slope factor. This exponent is related to, but not identical to, the Hill slope of the agonist concentration-response curve. Substitution of equation 3 for $S$ in equation 15 above followed by simplification yields:

$$response = \frac{X^m M_{sys}}{X^m + \frac{(X + K_{obs})^m}{\tau_{obs}{}^m}} \qquad 16$$

in which

$$K_{obs} = pK_X \qquad 17$$

$$\tau_{obs} = q\tau \qquad 18$$

$$\tau = \frac{\varepsilon R_T}{K_E} \qquad 19$$

It is useful to define the term *relative activity* (*RA*) of the agonist in the presence of the allosteric drug as:

JPET Fast Forward. Published on July 26, 2005 as DOI: 10.1124/jpet.105.090886
This article has not been copyedited and formatted. The final version may differ from this version.



$$RA = \frac{\tau_{obs} K_{obs}'}{\tau_{obs}' K_{obs}} \qquad 20$$

in which $\tau_{obs}$' and $K_{obs}$' denote the $\tau_{obs}$ and $K_{obs}$ values of the agonist in the absence of the allosteric drug. By making the appropriate substitutions for $K_{obs}$ and $\tau_{obs}$ (equations 17 and 18, respectively), it can be shown that equation 20 simplifies to equation 12. Also, it can be shown by substitution of equation 4 for *p* in equation 17 that the observed dissociation constant of the agonist ($K_{obs}$) in the presence of the allosteric drug divided by that measured in its absence ($K_{obs}$') is equivalent to:

$$\frac{K_{obs}}{K_{obs}'} = \frac{\left(1 + A/K_A\right)}{\left(1 + A/\alpha K_A\right)} \qquad 21$$

In situations where the exponent *m* in equation 16 equals one, the Hill slope is also equal to one (*n* = 1), and equation 16 reduces to:

$$response = \frac{XE_{\max}}{X + EC_{50}} \qquad 22$$

in which

$$E_{\max} = \frac{q\tau M_{sys}}{q\tau + 1} \qquad 23$$

$$EC_{50} = \frac{pK_X}{q\tau + 1} \qquad 24$$

When the Hill slope is equal to one, it is possible to estimate the *relative activity* (*RA*) of the agonist in the presence of the allosteric drug as:

$$RA = \frac{E_{\max} EC_{50}'}{E_{\max}' EC_{50}} \qquad 25$$

in which $EC_{50}$' and $E_{max}$' denote the $EC_{50}$ and $E_{max}$ values of the agonist in the absence of the allosteric drug and $EC_{50}$ and $E_{max}$ denote those measured in the presence of the allosteric drug. By making the appropriate substitutions for the various $EC_{50}$ and $E_{max}$ values (equations 23 and 24, respectively), it can be shown that equation 25, like equation 20, also simplifies to equation 12.

The use of equations 20, 21 and 25 in the analysis of allosteric effects in functional assays is described below under "Results."

# RESULTS

## Simulation of Allosterism in Functional Assays

The influence of allosteric modulators on the agonist concentration-response curve has been simulated by Kenakin (Kenakin, 1997) and Christopolous (Christopoulos, 2000) for a variety of conditions. These simulations and the theory for allosterism (Ehlert, 1988a) show that an allosteric modulator causes a concentration-dependent change in the agonist concentration-response curve. The magnitude of this change approaches a limit with high concentrations of the modulator. Allosteric changes in affinity are manifest as a parallel shift in the agonist concentration-response curve along the abscissa, whereas a modulation in efficacy is usually manifest as a shift or both a shift and change in the maximal response, depending upon the receptor reserve. Below, four simulations are shown to provide examples for the analysis of allosteric interactions.

*Allosteric modulator causing a decrease in both agonist affinity and efficacy*: The behavior of allosterism in functional assays can be appreciated by using equation 16 to generate agonist concentration-response curves in the presence of an allosteric drug having differential effects on agonist affinity and intrinsic efficacy. Figure 1*a-c* shows the effect of an allosteric drug causing a maximal 90% reduction in intrinsic efficacy ($ß = 0.1$) and observed affinity (10-fold increase in $K_{obs}$; $\alpha = 10$) for a response exhibiting a Hill slope ($n$) of one ($m = n = 1$). When there is little receptor reserve, increasing concentrations of the allosteric inhibitor cause a shift to the right and a decrease in the maximal response of the agonist concentration-response curve (Figure 1*a*). However, with an intermediate receptor reserve (see Figure 1*b*) there is less of a decline in $E_{max}$ and a greater shift to the right in the agonist concentration-response curve. With a large receptor reserve (Figure 1*c*), there is practically no decrease in $E_{max}$ and a maximal 100-fold shift to the right in the agonist concentration-response curve. The $EC_{50}$ and $E_{max}$ values of the agonist in the

presence of different concentrations of the allosteric inhibitor were estimated by nonlinear regression analysis of the data according to equation 13, and these values are listed in Table 1 for the data shown in Figures 1*a*-*c*.

To investigate the influence of the Hill slope on the behavior of allosterism, the effects of an allosteric drug essentially identical to that described for Figure 1*a*-*c* were simulated, but with the response of the agonist exhibiting a Hill slope (*n*) greater than one. This change was accomplished by setting the transducer slope faction in the operational model (*m*) equal to two. As shown in Figure 2*a*-*c*, behavior generally consistent with that observed in Figure 1*a*-*c* was observed. The effects of the allosteric inhibitor on the $EC_{50}$ and $E_{max}$ values of the agonist concentration-response curves shown in Figure 2 are listed in Table 2.

*Allosteric modulator causing an increase in both agonist affinity and efficacy*: The effects of an allosteric modulator causing both an increase in affinity and intrinsic efficacy of the agonist are shown in Figures 3*a*-*c*. In these simulations the maximal increases in affinity and efficacy were both ten-fold (i.e., $\alpha = 0.1$ and $ß = 10$), and the response exhibited a Hill slope (*n*) of one ($m = n = 1$). When there is little receptor reserve, increasing concentrations of the allosteric enhancer cause a shift to the left and an increase in the maximal response of the agonist concentration-response curve (Figure 3*a*). However, with an intermediate receptor reserve (see Figure 3*b*) there is a very small increase in $E_{max}$ and a greater increase in potency. With a large receptor reserve (Figure 3*c*), there is essentially no change in $E_{max}$ and a maximal 100-fold shift to the left in the agonist concentration-response curve. The effects of the allosteric enhancers on the $EC_{50}$ and $E_{max}$ values for all of the curves show in Figure 3*a*-*c* are listed in Table 3.

*Allosteric modulator having opposite effects on agonist affinity and efficacy*: The effects of an allosteric modulator causing equal and opposite modulation of agonist affinity and intrinsic efficacy were simulated. Figure 4*a* - *c* shows the effects of an allosteric modulator causing a maximal ten-fold increase in agonist affinity ($\alpha = 0.1$) and a maximal 90% reduction in agonist

JPET Fast Forward. Published on July 26, 2005 as DOI: 10.1124/jpet.105.090886
This article has not been copyedited and formatted. The final version may differ from this version.



efficacy ($ß = 0.1$) with the response exhibiting a Hill slope ($n$) of one ($m = n = 1$). When the receptor reserve is low (Figure 4*a*), the allosteric modulator causes a concentration-dependent decrease in both the $E_{max}$ and $EC_{50}$ values, so that the concentration response curve shifts to the left with a lowered maximum. Similar effects are observed when the receptor reserve is intermediate. However, when the receptor reserve is great, the allosteric inhibitor has little effect on the concentration-response curve because the reduction in efficacy is offset by an equivalent increase in affinity. The effect of the allosteric modulator on the $EC_{50}$ and $E_{max}$ values of the data simulated in Figure 4 are listed in Table 4.



Methods for the analysis of allosterism in functional assays

The methods for the analysis of allosterism presented here can be divided into two main categories, based on the application of the operational model and the null method described under "Methods." These approaches are described below in Sections 1 and 2, respectively, where they are applied in the analysis of the simulated data in Figures 1 – 4. In Section 3, a set of experimental data from the literature is analyzed.

Section 1: Operational Model:

The application of the operational model to the analysis of allosterism in functional assays involves three steps: 1) estimation of the *RA* values of the agonist in the presence of different concentrations of the allosteric modulator, 2) estimation of the $K_{obs}/K_{obs}$' ratios in the presence of different concentrations of the allosteric modulator, and 3) nonlinear regression analysis of the foregoing *RA* values and $K_{obs}/K_{obs}$' ratios according to equations 12 and 21, respectively. This analysis ultimately yields estimates of $K_A$ and $\gamma$ (equation 12) as well as $\alpha$ (equation 21), and hence $ß$, since $ß = \gamma/\alpha$. In the case where the Hill slopes of the agonist concentration-response curves do not differ significantly from one, it is possible to estimate the

*RA* values from the $E_{max}$ and $EC_{50}$ values of the concentration-response curves. Thus, in this instance, the concentration-response curves can be analyzed independently, using a nonlinear regression program (e.g., Prism, GraphPad Software, Inc., San Diego, CA) to estimate the $EC_{50}$ and $E_{max}$ values of each curve by fitting the standard equation for a sigmoidal dose-response curve having a Hill slope of one (equation 22) to the data. In situations where the Hill slopes differ from one, the *RA* values are estimated from the $\tau_{obs}$ and $K_{obs}$ values. These latter values can only be estimated by global nonlinear regression analysis according to equation 16, which involves analyzing the all of the curves measured at different amounts of allosteric modulator simultaneously, sharing estimates of $M_{sys}$ and $m$ among the curves. Similarly, estimation of the cooperativity factor $\alpha$ always involves global nonlinear regression analysis of all of the concentration response curves, regardless of the estimate of the Hill slope.

*Estimation of $K_A$ and $\gamma$ when the Hill slope is equivalent to one:* Since the agonist concentration-response curves shown in Figure 1*a* - *c* all exhibit Hill slopes of one, accurate estimates of the relative activity (*RA*) of the agonist can be estimated from the $E_{max}$ and $EC_{50}$ values using equation 25. These *RA* values are listed in Table 1 for the different concentrations of allosteric modulator. Figure 5*a* shows the Log *RA* values plotted against the Log of the concentration of allosteric modulator for the data from Figure 1*a*. In the presence of maximally effective concentrations of the allosteric modulator, the plot approaches an asymptote corresponding to the maximal combined change in observed affinity ($\alpha$) and intrinsic efficacy (ß) of the agonist. This combined effect on affinity and efficacy is denoted as $\gamma$ and is equivalent to ß/$\alpha$ (see equation 13). The Log form of equation 12 was fitted to the data by nonlinear regression analysis, which yielded estimates of $10^{-5}$ M and 0.01 for the $K_A$ and $\gamma$, respectively. These estimates are essentially identical to those used in simulating the data in the first place, demonstrating that the nonlinear regression method provides accurate estimates of the allosteric parameters of the modulator. The same procedure was used to analyze the simulated data in Figure 1*b* and *c*, and identical results were obtained. This result was expected since the only difference among the

JPET Fast Forward. Published on July 26, 2005 as DOI: 10.1124/jpet.105.090886
This article has not been copyedited and formatted. The final version may differ from this version.



plots in Figure 1*a* - *c* is the receptor reserve ($\tau$), and not the parameters of the allosteric modulator.

The functional data in Figure 3 for the allosteric modulator causing an increase in agonist affinity and efficacy can be analyzed in a manner analogous to that described above for the allosteric inhibitor in Figure 1 because both sets of data exhibit Hill slopes of one. Figure 5*c* shows a plot of the *RA* values (see Table 3) of the agonist plotted against the log of the allosteric modulator concentration for the data in Figure 3*a* - *c*. Regression analysis of the data according to equation 12 yielded estimates of $10^{-5}$ M and 100 for $K_A$ and $\gamma$, respectively. These values are identical to those used in the simulation of the data.

The functional data in Figure 4*a* - *c* can also be analyzed in a manner similar to that described for Figure 1*a* - *c*. Since the Hill slopes of the curves are equal to one, the *RA* values can be calculated according to equation 25, and these values are listed in Table 4. Figure 5*e* shows that the plot of Log *RA* against Log *A* yield a horizontal line at *RA* = 1. Thus, it is impossible to estimate $K_A$ from this plot, since any value of $K_A$ will yield a best fit of equation 12 to the data as long as $\gamma = 1$. In this case where $\alpha/ß = 1$, the $K_A$ value can be estimated through the analysis of the $K_{obs}$ values as described in the next section.

*Resolution of $\gamma$ into its $\alpha$ and ß components when the Hill slope is equivalent to one:* To discriminate between the modulatory effects of the allosteric agent on the observed dissociation constant and intrinsic efficacy of the agonist receptor complex, it is necessary to fit the operational model (equation 16) to all of the agonist concentration-response curves with varying allosteric modulator simultaneously. With regard to the data in Figure 1, regression analysis is done sharing the estimate of $M_{sys}$ among all of the curves and estimating unique values of $K_{obs}$ and $\tau_{obs}$ for each curve. Since all of the curves have Hill slopes of one, the exponent *m* can be removed from equation 16 or constrained at a constant value of one. Global nonlinear regression analysis of the data in Figure 1*a* yielded an estimate of 1.0 for $M_{sys}$, essentially the same as that used in the simulation of the data. The values of $\tau_{obs}$ and $K_{obs}$ for the various concentrations of

allosteric modulator are listed in Table 1. The relative activity (*RA*) values of the agonist can also be estimated from the $\tau_{obs}$ and $K_{obs}$ values for each concentration of allosteric modulator using equation 20, and these are also listed in Table 1. These *RA* values are essentially identical to those estimated from the $E_{max}$ and $EC_{50}$ values of the agonist (compare the last two columns in Table 1). Figure 5*b* shows a plot of the Log ratio ($K_{obs}/K_{obs}$') against the Log concentration of the allosteric modulator. It can be seen that this ratio reaches a plateau corresponding to $\alpha$ at high concentrations of allosteric modulator. Nonlinear regression analysis was used to fit the Log form of equation 21 to the data, which yielded estimates of $10^{-5}$ M and 10 for $K_A$ and $\alpha$, respectively. This estimate of $K_A$ is identical to that estimated from the *RA* values shown in Figure 5*a* and that used in the simulations, and the estimate of $\alpha$ is equivalent to that used in the simulations. Knowing $\gamma$ and $\alpha$, it is possible to estimate ß by rearrangement of equation 13 ($\gamma = ß/\alpha$), which yields an estimate of 0.1 for ß. This value is identical to that used in the simulations.

A similar analysis was done to estimate the $\tau_{obs}$ and $K_{obs}$ values for the concentration-response curves shown in Figure 1*b*, and these parameters are also listed in Table 1. The corresponding *RA* values were estimated (see Table 1), and found to be identical to those estimated from the curves in Figure 1*a*. Consequently, plots identical to those shown in Figure 5*a* and *b* were derived for the curves in Figure 1*b*, and the same values for $K_A$, $\alpha$, ß and $\gamma$ were estimated.

Under normal circumstances, where actual experimental data are analyzed, it would be difficult to obtain unique values of $\tau_{obs}$ and $K_{obs}$ for each curve shown in Figure 1*c* because all of the $E_{max}$ values of the curves are approximately the same. However, with the simulated data in Figure 1c, it is possible to obtain these estimates because the data have no error and there are actually small differences in the $E_{max}$ values. Regardless, in the situation of little change in $E_{max}$, it is always possible to obtain accurate estimates of the ratio of the two parameters (i.e., $\tau_{obs}/K_{obs}$), even though estimation of the individual values may be impossible. The nonlinear regression method for obtaining this ratio is described below in connection with Figure 6. As described in the next section, it is possible to estimate the *RA* values from these ratios, and these

JPET Fast Forward. Published on July 26, 2005 as DOI: 10.1124/jpet.105.090886
This article has not been copyedited and formatted. The final version may differ from this version.



estimates are listed in Table 1. The estimates of $\tau_{obs}$ and $K_{obs}$ for the data in Figure 1*c* have been omitted from Table 1 because they would be difficult to estimate in experiments with data having moderate experimental error.

The approach described for the estimation of $\alpha$ from the data in Figure 1 was applied to the data in Figures 3 and 4, and the results are summarized in Tables 3 and 4. Figure 5*d* shows the ratio of $K_{obs}$ values plotted against the log of the allosteric enhancer concentration for the data in Figures 3*a* and *b*. Regression analysis (equation 21) yielded estimates of $10^{-5}$ M and 0.1 for $K_A$ and $\alpha$, respectively. Knowing $\gamma$ and $\alpha$, it is possible to estimate a value of 10 for ß using equation 13. Figure 5*f* shows a plot of the Log ratio ($K_{obs}/K_{obs}$') against Log *A* for the data in Figures 4*a* and *b*. Regression analysis according to equation 21 yielded estimates of $10^{-5}$ M and 0.1 for $K_A$ and $\alpha$, respectively. Knowing that the horizontal plot in Figure 5*e* with $RA = 1$ implies that $\gamma = 1$, it is possible to estimate that ß = 0.1 by rearrangement of equation 13. It is impossible to estimate any allosteric parameters from the data in Figure 4*c* because the allosteric modulator has little or no effect on the concentration-response curve. This situation occurs because the allosteric effects on affinity and intrinsic efficacy are equal and opposite. When there is a large receptor reserve, the ten-fold reduction in intrinsic efficacy is manifest as a ten-fold shift to the right in the concentration-response curve, whereas the ten-fold increase in affinity causes the opposite effect, resulting in no net effect.

*Estimation of allosteric parameters when the Hill slope differs from one and there is a modulation of $E_{max}$:* To analyze the data shown in Figure 2 according to the operational model, it is inaccurate to estimate agonist *RA* from their $EC_{50}$ and $E_{max}$ values according to equation 25 because the Hill slopes of the concentration-response curve differ from 1. Consequently, equation 16 was fitted to all of the concentration response-curves simultaneously, sharing the estimate of $M_{sys}$ and the exponent *m* among the curves and estimating unique values of $\tau_{obs}$ and $K_{obs}$ for each curve. The global estimates of $M_{sys}$ and *m* from regression analysis were 1.0 and 2.0 for $M_{sys}$ and *m*, respectively. These values are identical to those used in the simulations. The

estimates of $\tau_{obs}$ and $K_{obs}$ were used to calculate the agonist *RA* values (see equation 20). These *RA* estimates are listed in Table 2 and are essentially the same as those listed in Table 1 for the curves shown in Figure 1*a* and *b*. This result was expected because the only difference between the parameters for the data in Figure 1*a* - *c* and Figure 2*a* - *c* is the value of *m*, but not any of the other parameters, including the *RA* values. Consequently, analysis of the *RA* values for Figures 2*a* and *b* yields plots essentially identical to those shown in Figures 5*a* and *b*, and the $K_A$, $\alpha$ and ß estimates for the allosteric drug were $10^{-5}$ M, 10 and 0.1, respectively.

*Estimation of allosteric parameters when the Hill slope differs from one and there is no modulation of $E_{max}$*: Since the receptor reserve is great for Figure 2*c* and all of the agonist concentration-response curves exhibit nearly the same $E_{max}$, numerous combinations of $\tau_{obs}$ and $K_{obs}$ all yield the same least squares fit. Nevertheless, it is possible to estimate the ratio of $\tau_{obs}/K_{obs}$ for each curve shown in Figure 2*c*. A least squares fit can be obtained when the value of $K_{obs}$ is equal to or greater than the larger of the two constants, $K_X$ or $\alpha K_X$. Thus, the best fit can be obtained by constraining $K_{obs}$ as a constant at any arbitrary value equal to or greater than the true value of $\alpha K_X$ ($10^{-4}$ M) and estimating unique values of $\tau_{obs}$ for each of the curves. A summary of this analysis is illustrated in Figure 6, which shows the best fitting parameter estimates for various values of $K_{obs}$ between $10^{-8}$ M and $10^{-1}$ M as well as the residual sum of squares (*RSS*). The ordinate scale on the left corresponds to the various parameter estimates, whereas that on the right corresponds to *RSS*. The data in Figure 6 are from the concentration-response curve simulated in the presence of $10^{-4}$ M *A*; analogous plots can be made for the data simulated at the other concentrations of *A*. The estimate of *RSS* in the figure is based on all of the curves, not just the one simulated at $A = 10^{-4}$ M. As the constrained value of $K_{obs}$ increases to $10^{-4}$, *RSS* approaches a minimum plateau and remains at this best fitting level with a further increase in $K_{obs}$ no matter how large. Thus, it can be seen that a least squares fit is obtained once the value of $K_{obs}$ is equal to or greater than $\alpha K_X$ ($10^{-4}$). As the value of $K_{obs}$ increases, the estimate of $\tau_{obs}$ increases in a proportional fashion so that the ratio of the two estimates ($\tau_{obs}/K_{obs}$)

is constant (Figure 6). Thus, the best fitting estimate of the ratio $\tau_{obs}/K_{obs}$ can be obtained by constraining $K_{obs}$ to an arbitrarily high constant value and estimating the other parameters that minimize *RSS*. Using this approach, the ratio of $\tau_{obs}/K_{obs}$ was estimated for each of the curves shown in Figure 2*c*. Alternatively, it is possible to set $\tau_{obs}$ as a constant and estimate the value of $K_{obs}$ that gives the least squares fit (analysis not shown).

Knowing the ratio of $\tau_{obs}/K_{obs}$ for each of the curves shown in Figure 2*c*, it is possible to estimate their respective *RA* values by dividing the ratio estimated in the presence of a given concentration of *A* by the corresponding ratio obtained for the control curve. In other words, if the $\tau_{obs}/K_{obs}$ ratio of one curve is divided by the corresponding ratio for the control curve ($\tau_{obs}'/K_{obs}'$) then the following ratio ($\tau_{obs}K_{obs}'/\tau_{obs}'K_{obs}$) is obtained, which is equivalent to the *RA* value (see equation 20). The *RA* values for the data in Figure 2*c* were estimated in this manner and are listed in Table 2. These values are identical to those estimated for the data in Figures 1*a* - *c* and Figures 2*a* and *b*; consequently, regression analysis of these data according to equation 20 yields a plot identical to that shown in Figure 5*a* with $K_A$ and $\gamma$ estimates of $10^{-5}$ M and 0.01, respectively. Since it was impossible to estimate unique $K_{obs}$ values for each of the curves shown in Figure 2*c*, it was impossible to separate $\gamma$ into it's $\alpha$ and ß components. As described above, it is impossible to make this distinction when the allosteric inhibitor has no influence on the $E_{max}$ of the concentration-response curve.

It is informative to estimate the *RA* values of the data shown in Figure 2 from the $E_{max}$ and $EC_{50}$ values according to equation 25. As described above, this equation is only appropriate for conditions when the Hill slopes of the agonist concentration-response curve are equal to one. When these estimate were made, and the data analyzed according to the plots shown in Figure 5*a* and *b*, estimates of 5.5 x $10^{-6}$ M and 0.00073 (Figure 2*a*) and 9.21 x $10^{-6}$ M and 0.0037 (Figure 2*b*) were made for $K_A$ and $\gamma$, respectively. Thus, there is substantial error in these parameters estimates, which should equal $10^{-5}$ M and 0.01. However, when this method was used to analyze the data in Figure 2*c*, values of $10^{-5}$ M and 0.0090 were estimated for $K_A$ and $\gamma$, respectively. Note that the latter value of $K_A$ is correct, whereas the estimate of $\gamma$ is only off by 10%. Thus,

when the allosteric inhibitor has no influence on $E_{max}$ it is possible to estimate the *RA* values according to equation 25, even if the Hill slopes differ from 1. This conclusion seems reasonable because the two different methods for calculating the RA value (equations 20 and 25) yield similar estimates for the data in Figure 2*c* but not for those of Figures 2*a* and *b* (Compare the last two columns of Table 2). Note that when the allosteric inhibitor has no effect on the $E_{max}$, the estimation of *RA* from equation 25 can be simplified to:

$$RA = \frac{EC_{50}'}{EC_{50}} \qquad 26$$

Figure 7 shows the ratio of $EC_{50}$ values of the agonist in the presence of the allosteric drug divided by that measured in its absence plotted against the Log of the allosteric drug concentration for the data from Figure 2*c*. Nonlinear regression analysis of the data according to the Log form of equation 20 yielded estimates of $10^{-5}$ M and 0.009 for $K_A$ and $\gamma$, respectively, as described above.

In summary, it can be concluded that whenever an allosteric modulator is without effect on $E_{max}$, only $K_A$ and $\gamma$ can be estimated. Under these conditions, one can estimate the *RA* values from Equation 25 or 26 even if the Hill slope differs from one. Equation 12 can be fitted to the data by nonlinear regression analysis to obtain estimates of $K_A$ and $\gamma$. It is unnecessary to perform the complicated regression analysis summarized in Figure 6 to estimate the *RA* values in this situation. Nevertheless, this analysis has been presented here to illustrate the relationship among the various parameter estimates in this situation.

Section 2: Null Method

An advantage of the null method for the analysis of allosteric interactions is that it can be applied to agonist concentration-response curves that deviate from logistic behavior. Nevertheless, the method will be used here to analyze the logistic curves shown in Figures 1 and 3. The null method involves three steps: 1) estimation of equiactive concentrations of agonist in

the absence (*X*) and presence (*X'*) of the various concentrations of the allosteric modulator, 2) global nonlinear regression analysis of the Log equiactive agonist concentrations to obtain estimates of the ratio *q/p* (*RA* values; see equation 11) of the agonist in the presence of different concentrations of the allosteric modulator, and 3) nonlinear regression analysis of the foregoing *RA* values according to equation 12. This analysis yields estimates of $K_A$ and $\gamma$.

*Allosteric modulator causes a reduction in* $E_{max}$: Figure 8 shows the application of this method for the data in Figure 1*a*. Since the allosteric modulator causes a reduction in the $E_{max}$ of the agonist, the agonist concentrations (*X*) are interpolated from the control concentration-response curve that yield responses equivalent to those elicited by the agonist concentrations (*X'*) used in the presence of the allosteric modulator (see Figure 8*a* for the data simulated at $A = 10^{-3}$ M). These pairs of equiactive agonist concentrations are then plotted on a Log scale as shown in Figure 8*b*. Each curve in Figure 8*b* corresponds to a different allosteric modulator concentration. These curves were analyzed simultaneously by global nonlinear regression analysis of the data according to the Log form of equation 9, with the estimate of $K_X$ shared among all the curves and unique values of *p* and *q* estimated for each curve. However, it is possible to estimate numerous combinations of $K_X$, *p* and *q* that yield the same least squares fit for each curve. Using an approach analogous to that described above in connection with Figure 6, it is possible to estimate the ratio *q/p* (*RA*; see equation 11), by constraining $K_X$ to a constant and determining the values of the other parameters that minimize *RSS*. Figure 8*c* shows the results of regression analysis for the data simulated at $A = 10^{-3}$ M. Over the range of $K_X$ values shown ($10^{-9}$ - $10^{-1}$), RSS was insignificant and depended only on the criteria used for convergence of the nonlinear regression algorithm and not on $K_X$. Analogous behavior was observed for the data simulated at the other concentrations of *A*. Using this approach, various values of *RA* can be estimated at various the concentrations of the allosteric modulator (*A*). The resulting Log *RA* values are plotted against Log *A* and analyzed by nonlinear regression analysis according to equation 11. The results yielded a plot identical to that shown in Figure 5*a*, and values of $10^{-5}$ M and 0.01 were estimated

for $K_A$ and $\gamma$, respectively. These values are identical to those used in the simulation of the data in Figure 1*a*. The data in Figure 1*b* were analyzed in a similar fashion and the same estimates of $\gamma$ and $K_A$ were obtained (i.e., 0.01 and $10^{-5}$ M, respectively).

It is also possible to use the same strategy for the simulated data in Figure 1*c*; however, since the data exhibit little or no change in $E_{max}$ with allosteric modulation, it is necessary to constrain both $K_X$ and $p$ as constants and analyze all of the data simultaneously by global nonlinear regression analysis (equation 9) to obtain $q$ values for each of the curves. By dividing the estimates of $q$ value by the constant value of $p$, it is possible to obtain the $RA$ estimates for each curve, and hence, the values of $\gamma$ and $K_A$ by regression analysis according to equation 12. When this was done, a plot identical to that shown in Figure 5*a* was obtained as well as the same estimates of $\gamma$ and $K_A$ (0.01 and $10^{-5}$ M, respectively). Regardless, this complicated analysis is probably unnecessary because the $RA$ values can be estimated accurately from $EC_{50}$ values according to equation 26 when there is little change in $E_{max}$ with the allosteric modulator. Presumably, this situation would apply to non-logistic agonist concentration-response curves.

*Allosteric modulator causes an increase in $E_{max}$*: In situations where the allosteric modulator causes an increase in the $E_{max}$ of the agonist, it is possible to analyze the data according to null equation 10. However, in this instance, where the concentration-response curve in the presence of the allosteric modulator has a greater $E_{max}$ than that measured in its absence, the $X'$ values are interpolated from the curve measured in the presence of the allosteric inhibitor that yield responses equivalent to those generated by the concentrations ($X$) of the control concentration-response curve. Using this approach and an overall strategy analogous to that just described in the preceding paragraph, it is possible to estimate the $\gamma$ and $K_A$ values for the allosteric enhancer shown in Figures 3*a* – *c*. However, an important difference is the range of values over which the parameter $K_X$ can be constrained as a constant for global nonlinear regression analysis. This range was found to be $K_X \leq 10^{-5}$ for the data in Figure 3. When this analysis was done, plots

identical to that shown in Figure 5*c* were obtained, and values of 100 and $10^{-5}$ M were estimated for $\gamma$ and $K_A$, respectively, which are equivalent to those used in simulating the data.

Using the null approach, it is also possible to estimate the $\gamma$ and $K_A$ values of the other allosteric modulators simulated above, with the exception of the data in Figure 4. In this case, the plot of *RA* against Log *A* yields a horizontal line at *RA* = 1 as shown in Figure 5*e*. As described above, it is impossible to estimate $K_A$ from this figure, only $\gamma$. In summary, if the allosteric modulator causes a decrease in $E_{max}$, the approach describe in connection with Figure 10 is used, whereas if an increase in $E_{max}$ is observed, the approach described in the preceding paragraph is used.

Section 3: Experimental data

The methods based on the operational model were applied to experimental data to determine the impact of experimental error on the estimates of allosteric parameters. Figure 9*a* shows the results of a prior study in which the influence of gallamine on muscarinic receptor mediated inhibition of adenylyl cyclase activity was measured in homogenates of the rat myocardium (Ehlert, 1988b). This preparation is known to contain a relatively homogeneous population of $M_2$ muscarinic receptors (Hammer et al., 1986). Gallamine is a neuromuscular blocking agent long known to cause sinus tachycardia (Walton, 1950) through a mechanism involving an inhibition of postjunctional muscarinic receptors (Riker and Wescoe, 1951). The mechanism was later shown to be allosteric in functional studies on isolated beating hearts (Clark and Mitchelson, 1976) and in muscarinic receptor binding assays (Stockton et al., 1983).

As shown in Figure 9*a*, gallamine caused a concentration-dependent shift to the right in the agonist concentration-response curve with little change in $E_{max}$. Regression analysis of each curve according to logistic equation 14 yielded the estimates of $EC_{50}$, $E_{max}$ and *n* (Hill slope), and these values are listed in Table 5. The results show that the agonist concentration-response curves exhibit low Hill slopes (approximately 0.7 – 1.0) and that there is little change in $E_{max}$. In

JPET Fast Forward. Published on July 26, 2005 as DOI: 10.1124/jpet.105.090886
This article has not been copyedited and formatted. The final version may differ from this version.



this situation, it is only possible to estimate $K_A$ and $\gamma$; it is impossible to resolve $\gamma$ into it's $\alpha$ and ß components from these data alone (see analysis of the data in Figures 1*c* and 3*c*). Accordingly, the *RA* value of the agonist can be estimated easily by calculating the ratio of $EC_{50}$ values measured in the presence of gallamine divided by that measured in its absence as described above in equation 26. Nevertheless, the *RA* values were estimated using the operational model so that the influence of experimental error on these estimates might be appreciated. Normally, this method would only be required in situations where the allosteric modulator influences the $E_{max}$.

The data were analyzed by global nonlinear regression analysis according to equation 16 using the procedure described above in connection with Figure 6 for the estimation of *RA* values. Regression analysis was done sharing the estimates of $M_{sys}$ and $m$ among the curves and constraining $K_{obs}$ as a constant so that the ratio $\tau_{obs}/K_{obs}$ could be estimated. A summary of the analysis of the data at $10^{-4}$ M gallamine is shown in Figure 9*b* where the logarithm of the parameter estimates are plotted against $K_{obs}$, which was constrained to various fixed values during regression analysis. A least squares fit was obtained over the range $K_{obs} > 10^{-3}$ as shown by the minimum value for Log *RSS*. Over this range the estimates of $M_{sys}$, $m$ and the ratio $\tau_{obs}/K_{obs}$ were constant. This process was repeated for each curve in Figure 9*a*, and a least squares fit was always obtained over the domain $K_{obs} > 10^{-3}$. The estimates ± S.E. of $M_{sys}$ and $m$ were 55 ± 1.4 % inhibition and 0.68 ± 0.037, respectively. The *RA* values were calculated from the $\tau_{obs}/K_{obs}$ ratios estimated with $K_{obs}$ constrained to an arbitrarily high value (i.e., $10^{-2}$), and these estimates are also listed in Table 5 and plotted in Figure 9*b*. Regression analysis of the data according to equation 12 yielded estimates of $K_A$ and $\gamma$ of 0.62 µM and 0.019, respectively (mean ± S.E.M.: $pK_A$, 6.21 ± 0.15; Log $\gamma$ = -1.72 ± 0.16).

For heuristic purposes, the *RA* values were also estimated using equation 25. Generally, the use of equation 25 is restricted to data with Hill slopes of one, but as described above, it is applicable in situations where there is little change in $E_{max}$. These estimates were made for each experiment and the mean values of four experiments ± S.E.M. are listed in Table 5. The

JPET Fast Forward. Published on July 26, 2005 as DOI: 10.1124/jpet.105.090886
This article has not been copyedited and formatted. The final version may differ from this version.



corresponding Log *RA* values are also plotted against the Log of the gallamine concentration in Figure 9*c*. Regression analysis of the data according to equation 12 yielded estimates of $K_A$ and $\gamma$ of 0.56 μM and 0.025, respectively (mean ± S.E.M.: $pK_A$, 6.25 ± 0.21; Log $\gamma$ = -1.60 ± 0.21).

JPET Fast Forward. Published on July 26, 2005 as DOI: 10.1124/jpet.105.090886
This article has not been copyedited and formatted. The final version may differ from this version.



# DISCUSSION

The study of allosterism in functional assays provides potential information about the allosteric modulation of the intrinsic efficacy of the agonist-receptor complex. This information is important because the therapeutic effects of allosteric modulators depend on their modulation of both the affinity and intrinsic efficacy of the endogenous ligand. The theoretical basis for the present analysis was described in a prior report (Ehlert, 1988a), where it was shown that simple graphical techniques can be used to estimate the affinity of the allosteric modulator and its combined effects on the affinity and intrinsic efficacy ($\gamma$) of the agonist-receptor complex when the receptor reserve is great. Given the widespread availability of software for nonlinear regression analysis, the time seemed appropriate to reinvestigate this method and to apply it to all conditions. To this end, the concept of relative activity of the agonist (*RA*) is developed here and shown to be a robust measure of allosteric effects.

The present report shows that it is always possible to estimate the influence of the allosteric modulator on the *RA* value of the agonist. Regression analysis of the *RA* values according to the logarithmic form of equation 12:

$$Log(RA) = Log\left(\frac{1 + \gamma A/K_A}{1 + A/K_A}\right) \qquad 27$$

provides estimates of the dissociation constant ($K_A$) of the allosteric modulator as well as the product ($\gamma$) of its modulatory effects on the intrinsic efficacy (ß) and affinity ($1/\alpha$) of the agonist-receptor complex. In situations where the Hill slopes of the agonist concentration-response curves are equal to one, the *RA* values can be estimated easily from the $EC_{50}$ and $E_{max}$ values (see equation 21). If the allosteric modulator has no influence on the $E_{max}$ of the agonist, it is impossible to determine the individual components of $\gamma$ ($\alpha$ and ß) unless an independent estimate of $\alpha$ is made, perhaps through ligand binding analysis (see Lazareno et al. (1995)). If the allosteric modulator does influence the $E_{max}$ of the agonist, then it is possible to estimate the individual components $\alpha$ and ß as described above under Results. The method involves global

JPET Fast Forward. Published on July 26, 2005 as DOI: 10.1124/jpet.105.090886
This article has not been copyedited and formatted. The final version may differ from this version.



nonlinear regression analysis with the operational model (equation 15) to obtain individual estimates of $\tau_{obs}$ and $K_{obs}$.

For heuristic purposes, this analysis has emphasized the utility of the *RA* estimate in understanding allosteric interactions. Consequently, the Log *RA* value has been treated as the dependent variable in nonlinear regression analysis. However, this strategy might not be the best statistical approach when the *RA* value is estimated from the $EC_{50}$ and $E_{max}$ values in situations where the Hill slope is equivalent to one. For example, if there is error in the estimates of the $E_{max}$ and $EC_{50}$ values of the control concentration-response curve, then this error will introduce a systematic error in the *RA* estimates for all the concentration-response curves measured in the presence of the allosteric modulator. A better strategy might be to calculate Log ratio of the $E_{max}/EC_{50}$ values measured in the absence and presence of the various concentrations of the allosteric modulator and use the following equation to analyze the data by nonlinear regression analysis:

$$Log\left(\frac{E_{\max}}{EC_{50}}\right) = P + Log\left(\frac{1+\gamma A/K_A}{1+A/K_A}\right) \qquad 28$$

Regression analysis should yield estimate of $\gamma$, $K_A$ and $P$, the Log ratio of $E_{max}'/EC_{50}'$ for the control agonist concentration-response curve. The latter equation can be derived from equations 25 and 26, and it only applies to situations where the Hill slope of the concentrations response curves are equivalent to one. Also, when the Hill slope is equivalent to one and the allosteric modulator has no influence on $E_{max}$, the above equation reduces to that previously described (Ehlert, 1988b):

$$Log(EC_{50}) = Log(EC_{50}') + Log\left(\frac{1+A/K_A}{1+\gamma A/K_A}\right) \qquad 29$$

Regression analysis would yield estimates of $\gamma$, $K_A$ and the Log control $EC_{50}$ value. A similar statistical argument might seem appropriate when the *RA* values are estimated from $K_{obs}$ and $\tau_{obs}$ (i.e., error in the estimates of $K_X$ and $\tau$ will introduce a systematic error in the estimate of *RA*); however, this concern is unnecessary because the values of $K_X$ and $\tau$ ($K_{obs}'$ and $\tau_{obs}'$) are estimated by global nonlinear regression analysis (equation 10) of all of the agonist

concentration-response curves simultaneously. Thus, all of the data is considered in the estimation of $K_X$ and $\tau$ and not just the control data.

It should be apparent from the foregoing that it is possible to estimate the dissociation constant of the agonist ($K_X$) through the analysis of an allosteric modulator that influences the intrinsic efficacy of the agonist to such an extent that a change in $E_{max}$ is observed.

The present report also describes a null method, whereby the values of $K_A$ and $\gamma$ were determined by nonlinear regression analysis of pairs of equiactive agonist concentrations in the absence and presence of various concentrations of the allosteric modulator. This type of approach should be applicable in situations where the response of the agonist deviates from logistic behavior.

The estimates of the $K_A$ (0.56 – 0.62 μM) and $\gamma$(0.019 – 0.025) values for gallamine antagonism of the action of oxotremorine-M at $M_2$ muscarinic receptors made in this report by regression analysis of the Log *RA* values are in good agreement with those (0.52 μM and 0.020) made in a prior analysis of the same data utilizing regression analysis of the Log $EC_{50}$ values according to equation 29 above (Ehlert, 1988b). This agreement shows the feasibility of estimating *RA* values from experimental data. The estimate of the $K_A$ of gallamine reported here is also in good agreement with that (0.93 μM) estimated by antagonism of the negative inotropic effect of acetylcholine in the isolated, electrically driven, guinea pig atrium (Christopoulos, 2000) and by competitive inhibition of the binding of [$^3$H]N-methylscopolamine to myocardial muscarinic receptors (Stockton et al., 1983; Ehlert, 1988b) (0.77 and 1.1 μM, respectively).

In a prior report on the antagonism of the action of the highly efficacious agonist oxotremorine-M and the partial agonist BM-5 at cardiac $M_2$ muscarinic receptors by gallamine, the estimates of $\gamma$ were calculated to be 0.020 and 0.011, respectively (Ehlert, 1988b). In both cases, gallamine had little or no effect on the $E_{max}$ values of the agonists. Since BM-5 behaved as a partial agonist, any gallamine-induced change in the intrinsic efficacy of BM-5 should have been manifest as an alteration in $E_{max}$. The lack of this change indicates that $ß = 1$ and $\alpha = 0.011$, approximately, for the allosteric interaction between gallamine and BM-5 (i.e., $\gamma = \alpha/ß = 0.011$).

Additional proof for this hypothesis could be obtained if a similar estimate of the $\alpha$ value for the interaction between gallamine and BM-5 was obtained in ligand binding studies using the technique described by Lazareno and Birdsall (Lazareno and Birdsall, 1995).

The presumed lack of effect of gallamine on the intrinsic efficacy of BM-5 has important implications with regard to the action of gallamine and the number of ground and active states of the $M_2$ muscarinic receptor. In a simple two-state model, where there is only one active and one inactive state of the receptor, there should be a correlation between allosteric effects and the intrinsic efficacy of the primary ligand (Ehlert, 2000). However, gallamine has been shown to inhibit the binding of both agonists and antagonists to $M_2$ muscarinic receptors. Moreover, if gallamine reduces the affinity of BM-5 without influencing its intrinsic efficacy, this result implies the existence of another pair of ground and active states of the $M_2$ receptor that are selected by gallamine and whose affinities for BM-5 are both lower by the same amount so that the selectivity of BM-5 for the two states is the same, and hence, its efficacy unaltered (i.e., the ratio of microscopic affinity constants of BM-5 for the ground and active states are the same). Alternatively, a more complicated hypothesis involving a group of active and inactive states might explain the data.

Part of the analysis described herein is analogous to a method previously described for analyzing a series of concentration-response curves to different agonists with varying affinity and intrinsic efficacy. In that prior analysis, the concept of intrinsic relative activity (*IRA*) was developed (Ehlert et al., 1999; Ehlert and Griffin, 2001). This term denotes the product of the affinity and intrinsic activity of the agonist expressed relative to that of a standard agonist. This estimate is analogous to the *RA* value described here, which is a measure of the product of affinity and intrinsic efficacy of the agonist in the presence of the allosteric modulator relative to that measured in its absence.

Accurate measurements of the components of allosterism are important and likely to be more significant as the number of allosteric drugs used in therapeutics and research increases.

REFERENCES

Black JW and Leff P (1983) Operational models of pharmacological agonism. *Proc. Roy. Soc. Lond. B* **220**:141-162.

Burgen AS (1981) Conformational changes and drug action. *Fed. Proc.* **40**:2723-2728.

Christopoulos A (2000) Quantification of allosteric interactions at G protein-coupled receptors using radioligand binding assays, in *Current Protocols in Pharmacology* (Enna SJ ed), Wiley & Sons, New York.

Christopoulos A (2002) Allosteric binding sites on cell-surface receptors: novel targets for drug discovery. *Nat Rev Drug Discov* **1**:198-210.

Clark AL and Mitchelson F (1976) The inhibitory effect of gallamine on muscarinic receptors. *Brit. J. Pharmacol.* **58**:323-331.

Ehlert FJ (1986) 'Inverse agonists', cooperativity and drug action at benzodiazepine receptors. *Trends Pharmacol. Sci.* **7**:28-32.

Ehlert FJ (1988a) Estimation of the affinities of allosteric ligands using radioligand binding and pharmacological null methods. *Mol. Pharmacol.* **33**:187-194.

Ehlert FJ (1988b) Gallamine allosterically antagonizes muscarinic receptor-mediated inhibition of adenylate cyclase activity in the rat myocardium. *J. Pharmacol. Exp. Ther.* **247**:596-602.

Ehlert FJ (2000) Ternary Complex Model, in *Biomedical Applications of Computer Modeling* (Christopoulos A ed) pp 21-85, CRC Press, Boca Raton.

Ehlert FJ and Griffin MT (2001) Estimation of agonist activity and relative efficacy at G protein-coupled receptors: Mutational analysis and characterization of receptor subtypes. *Analytical Pharmacology* **2**:34-48.

Ehlert FJ, Griffin MT, Sawyer GW and Bailon R (1999) A simple method for estimation of agonist activity at receptor subtypes: comparison of native and cloned $M_3$ muscarinic

receptors in guinea pig ileum and transfected cells. *J. Pharmacol. Exp. Ther.* **289**:981-992.

Furchgott RF (1966) The use of β-haloalkylamines in the differentiation of receptors and in the determination of dissociation constants of receptor-agonist complexes. *Adv. Drug Res.* **3**:21-55.

Hall DA (2000) Modeling the functional effects of allosteric modulators at pharmacological receptors: an extension of the two-state model of receptor activation. *Mol. Pharmacol.* **58**:1412-1423.

Hammer R, Giraldo E, Schiavi GB, Monferini E and Ladinsky H (1986) Binding profile of a novel cardioselective muscarine receptor antagonist, AF-DX 116, to membranes of peripheral tissues and brain in the rat. *Life Sci.* **38**:1653-1662.

Kenakin TP (1997) *Pharmacologic analysis of Drug-receptor interaction*. Lippincott-Raven Publishers, Philadelphia.

Kenakin TP and Beek D (1982) In vitro studies on the cardiac activity of prenalterol with reference to use in congestive heart failure. *J. Pharmacol. Exp. Ther.* **220**:77-85.

Lazareno S and Birdsall NJ (1995) Detection, quantitation, and verification of allosteric interactions of agents with labeled and unlabeled ligands at G protein-coupled receptors: interactions of strychnine and acetylcholine at muscarinic receptors. *Mol. Pharmacol.* **48**:362-378.

Mackay D (1981) An analysis of functional antagonism and synergism. *Brit. J. Pharmacol.* **73**:127-134.

Riker WF, Jr. and Wescoe WC (1951) The pharmacology of Flaxedil, with observations on certain analogs. *Ann N Y Acad Sci* **54**:373-394.

Stephenson RP (1956) A modification of receptor theory. *Brit. J. Pharmacol.* **11**:379-393.

Stockton JM, Birdsall NJ, Burgen AS and Hulme EC (1983) Modification of the binding properties of muscarinic receptors by gallamine. *Mol. Pharmacol.* **23**:551-557.

Walton FA (1950) Flaxedil, a new curarizing agent. *Can Med Assoc J* **63**:123-129.

FOOTNOTES

[a] This work was supported by National Institutes of Health Grant 69829

Send reprint requests to:

Frederick J. Ehlert, Ph.D.

Department of Pharmacology

College of Medicine

University of California, Irvine

Irvine, California 92697-4625

Legends to Figures

Figure 1: Simulation of the effects of an allosteric modulator inhibiting both agonist affinity and intrinsic efficacy on the concentration-response curve to an agonist having a Hill slope ($n$) of one (i.e., $m = n = 1$). In these examples, the allosteric modulator causes both a maximal ten-fold reduction in the affinity ($\alpha = 10$) and intrinsic efficacy ($ß = 0.1$) of the agonist-receptor complex. Small ($\tau = 1$) (*a*), intermediate ($\tau = 10$) (*b*) and large ($\tau = 100$) (*c*) receptor reserves were simulated. The dissociation constant of the allosteric inhibitor ($K_A$) was $10^{-5}$ M and $M_{sys} = 1$. The concentrations of allosteric modulator are indicated in panel *a* for the entire figure.

Figure 2: Simulation of the effects of an allosteric inhibitor on the concentration-response curve to an agonist having a transducer slope factor in the operational model of two ($m = 2$). In this example, the allosteric modulator causes maximal ten-fold reductions in both affinity and intrinsic efficacy ($\alpha = 10$; $ß = 0.1$) of the agonist-receptor complex. Small ($\tau = 1$) (*a*), intermediate ($\tau = 10$) (*b*) and large ($\tau = 100$) (*c*) receptor reserves were simulated. The dissociation constant of the allosteric inhibitor ($K_A$) was $10^{-5}$ M and $M_{sys} = 1$. The concentrations of allosteric modulator are indicated in panel *a* for the entire figure.

Figure 3: Simulation of the effects of an allosteric modulator enhancing both agonist affinity and intrinsic efficacy on the concentration-response curve to an agonist having a Hill slope ($n$) of one ($m = n = 1$). In these examples, the allosteric modulator causes both a maximal ten-fold increase in only the affinity ($\alpha = 0.1$) and intrinsic efficacy ($ß = 10$) of the agonist-receptor complex. Small ($\tau = 1$) (*a*), intermediate ($\tau = 10$) (*b*) and large ($\tau = 100$) (*c*) receptor reserves were simulated. The dissociation constant of the allosteric inhibitor ($K_A$) was $10^{-5}$ M and $M_{sys} = 1$. The concentrations of allosteric modulator are indicated in panel *a* for the entire figure.

Figure 4: Simulation of the effects of an allosteric modulator on the concentration-response curve to an agonist having a Hill slope ($n$) of one ($m = n = 1$). In this example, the

allosteric modulator causes both a maximal ten-fold increase in affinity and a 10-fold decrease in intrinsic efficacy ($\alpha = 0.1$; $ß = 0.1$) of the agonist-receptor complex. Small ($\tau = 1$) (*a*), intermediate ($\tau = 10$) (*b*) and large ($\tau = 100$) (*c*) receptor reserves were simulated. The dissociation constant of the allosteric inhibitor ($K_A$) was $10^{-5}$ M and $M_{sys} = 1$. The concentrations of allosteric modulator are indicated in panel *a* for the entire figure.

Figure 5: Effect of allosteric modulators on the *RA* (*a*, *c* and *e*) and $K_{obs}$ (*b*, *d* and *f*) values of the agonist. The plots in *a* and *b* represent an analysis of the data shown in Figure 1*a* – *c* and 2*a* – *c*, and the estimates of *RA* and $K_{obs}$ are from Tables 1 and 2. The plots in *c* and *d* represent an analysis of the data shown in Figure 3*a* – *c*, and the estimates of *RA* and $K_{obs}$ are from Table 3. The plots in *e* and *f* represent an analysis of the data shown in Figure 4*a* – *c*, and the estimates of *RA* and $K_{obs}$ are from Table 4. The dashed lines in *a* and *c* denote the maximal effect of the allosteric modulator on the *RA* value ($\gamma$). The dashed lines in *b*, *d* and *f* denote the maximal shift ($\alpha$) of the allosteric modulator on the observed affinity of the agonist.

Figure 6: Summary of global nonlinear regression analysis of the data in Figure 2*c* at $A = 10^{-4}$ M according to equation 16. All of the curves in Figure 2*c* were fitted simultaneously sharing the estimate of *m* and $M_{sys}$ among the curves and constraining the value of $K_{obs}$ as a constant at various values between $10^{-5}$ and $10^{-1}$. Regression analysis was used to estimate the values of the various parameters in equation 16 that yielded the least squares fit to the data. The plot shows how the estimate of $\tau_{obs}$ for the data simulated at A = $10^{-4}$ M is proportional to $K_{obs}$ such that their ratio ($\tau_{obs}/K_{obs}$) remains constant at approximately $10^6$.

Figure 7: The influence of an allosteric inhibitor on the $EC_{50}$ value of an agonist when the receptor reserve is great ($\tau = 100$) and the transducer slope factor in the operational model is equal to two ($m = 2$). The ratio of the control $EC_{50}$ value divided by that measured in the presence of the allosteric modulator is plotted on a Log scale against the concentration of the allosteric modulator. The allosteric modulator causes a ten-fold reduction in the

affinity ($\alpha$ = 10) and intrinsic efficacy ($ß$ = 0.1) of the agonist receptor complex. The plot represents an analysis of the data shown in Figure 2*c*. The $EC_{50}$ values are from Table 2.

Figure 8: Estimation of the modulatory effects of an allosteric inhibitor using a null method. The data are from Figure 1*a*. *a*: Pairs of equiactive agonist concentrations in the absence and presence of the allosteric modulator are estimated. This plot is for the data simulated for $A = 10^{-3}$ M; a similar analysis was done for the other concentrations of allosteric modulator. *b*: The logarithms of the equiactive agonist concentrations are analyzed by nonlinear regression analysis using equation 9. The curves are analyzed simultaneously sharing the estimates of $K_X$ among the curves and estimating a unique value of *p* and *q* for each curve. *c*: Summary of nonlinear regression analysis for the data simulated at $A = 10^{-3}$ M. The value of $K_X$ was constrained as a constant over the range of values shown on the abscissa and the values of the other parameters that yielded the least squares fit to the simulated data were estimated by regression analysis as shown by the indicated curves. It can be seen that the estimates of *p* and *q* are proportional to one another such that their ratio (*q/p* or *RA*) remains constant over the range of $K_X$ values shown.

Figure 9: Analysis of the antagonism of oxotremorine-M-mediated inhibition of adenylyl cyclase activity by gallamine in homogenates of the rat myocardium. *a*: Adenylyl cyclase activity was measured in the presence of various concentration of both oxotremorine-M and gallamine. The data are from Ehlert (1988b). Mean values ± S.E.M. from four experiments are shown. *b*: Summary of global nonlinear regression analysis of the concentration-response curves shown in panel *a* at gallamine = $10^{-4}$ M according to equation 16. All of the curves were fitted simultaneously sharing the estimate of *m* and $M_{sys}$ among the curves and constraining the value of $K_{obs}$ as a constant at various values between $10^{-6}$ and $10^{0}$. Regression analysis was used to estimate the values of the various parameters in equation 16 that yielded the best least squares fit to the data. The plot shows how the estimate of $\tau_{obs}$ for the data simulated at gallamine = $10^{-4}$ M is proportional to $K_{obs}$ such that their ratio ($\tau_{obs}/K_{obs}$) remains constant at approximately 3.7 x $10^{4}$. *c*: Effect of

JPET Fast Forward. Published on July 26, 2005 as DOI: 10.1124/jpet.105.090886
This article has not been copyedited and formatted. The final version may differ from this version.



gallamine on the *RA* values of oxotremorine-M. The plots represent an analysis of the data shown in panel *a*, and the estimates of *RA* were calculated from the $K_{obs}$ and $\tau_{obs}$ values or the $E_{max}$ and $EC_{50}$ values listed in Table 5.

JPET Fast Forward. Published on July 26, 2005 as DOI: 10.1124/jpet.105.090886
This article has not been copyedited and formatted. The final version may differ from this version.



Table 1: Estimates of $EC_{50}$, $E_{max}$, Hill slope, $K_{obs}$ and $\tau_{obs}$ for the simulated data in Figures 1*a* – *c*. In this example the allosteric modulator causes a ten-fold reduction in both the affinity ($\alpha = 10$) and intrinsic efficacy ($ß = 0.1$) of the agonist-receptor complex.

| *Allosteric Modulator (M)* | $EC_{50}$ *(μM)* | $E_{max}$ *(%)* | *Hill Slope* | $K_{obs}$ *(μM)* | $\tau_{obs}$ | $\frac{E_{max} EC_{50}' \, a}{E_{max}' EC_{50}}$ *(RA)* | $\frac{\tau_{obs} K_{obs}' \, a}{\tau_{obs}' K_{obs}}$ *(RA)* |
|---|---|---|---|---|---|---|---|
| $\tau = 1$ | | | | | | | |
| 0 | 5.00 | 50 | 1.0 | 10.0 | 1.00 | 1.00 | 1.00 |
| $10^{-5}$ | 9.46 | 47.9 | 1.0 | 18.2 | 0.918 | 0.506 | 0.505 |
| $10^{-4}$ | 35.5 | 35.5 | 1.0 | 55.0 | 0.550 | 0.100 | 0.100 |
| $10^{-3}$ | 78.2 | 15.4 | 1.0 | 91.8 | 0.182 | 0.0197 | 0.0198 |
| $10^{-2}$ | 89.1 | 9.8 | 1.0 | 99.1 | 0.109 | 0.0110 | 0.0110 |
| $\tau = 10$ | | | | | | | |
| 0 | 0.908 | 90.9 | 1.0 | 10.0 | 10.0 | 1.00 | 1.00 |
| $10^{-5}$ | 1.79 | 90.2 | 1.0 | 18.2 | 9.18 | 0.504 | 0.505 |
| $10^{-4}$ | 8.47 | 84.6 | 1.0 | 55.0 | 5.50 | 0.100 | 0.100 |
| $10^{-3}$ | 32.5 | 64.5 | 1.0 | 91.8 | 1.82 | 0.0197 | 0.0198 |
| $10^{-2}$ | 47.3 | 52.1 | 1.0 | 99.1 | 1.09 | 0.0110 | 0.0110 |
| $\tau = 100$ | | | | | | | |
| 0 | 0.0991 | 99.0 | 1.0 | - | - | 1.00 | 1.00 |
| $10^{-5}$ | 0.196 | 98.9 | 1.0 | - | - | 0.504 | 0.505 |
| $10^{-4}$ | 0.984 | 98.2 | 1.0 | - | - | 0.100 | 0.100 |
| $10^{-3}$ | 4.79 | 94.8 | 1.0 | - | - | 0.0198 | 0.0198 |
| $10^{-2}$ | 8.32 | 91.6 | 1.0 | - | - | 0.0110 | 0.0110 |

(*Table 1 continued*)

JPET Fast Forward. Published on July 26, 2005 as DOI: 10.1124/jpet.105.090886
This article has not been copyedited and formatted. The final version may differ from this version.



[a] $EC_{50}$', $E_{max}$', $K_{obs}$' and $\tau_{obs}$' denote the corresponding parameter values of $EC_{50}$, $E_{max}$, $K_{obs}$ and $\tau_{obs}$ in the absence of allosteric modulator.

JPET Fast Forward. Published on July 26, 2005 as DOI: 10.1124/jpet.105.090886
This article has not been copyedited and formatted. The final version may differ from this version.



Table 2: Estimates of $EC_{50}$, $E_{max}$, Hill slope, $K_{obs}$ and $\tau_{obs}$ for the simulated data in Figures 2*a* – *c*. In this example the allosteric modulator causes a ten-fold reduction in both the affinity ($\alpha = 10$) and intrinsic efficacy ($ß = 0.1$) of the agonist-receptor complex.

| *Allosteric Modulator (M)* | $EC_{50}$ *(μM)* | $E_{max}$ *(%)* | *Hill Slope* | $K_{obs}$ *(μM)* | $\tau_{obs}$ | $\frac{E_{max} EC_{50}'}{E_{max}' EC_{50}}$ [a] | $\frac{\tau_{obs} K_{obs}'}{\tau_{obs}' K_{obs}}$ [a] *(RA)* |
|---|---|---|---|---|---|---|---|
| $\tau = 1$ | | | | | | | |
| 0 | 14.1 | 49.6 | 1.30 | 10.0 | 1.00 | 1.00 | 1.00 |
| $10^{-5}$ | 27.4 | 45.3 | 1.29 | 18.2 | 0.918 | 0.472 | 0.505 |
| $10^{-4}$ | 108 | 22.9 | 1.28 | 55.0 | 0.550 | 0.0606 | 0.100 |
| $10^{-3}$ | 216 | 3.14 | 1.25 | 91.8 | 0.182 | 0.0041 | 0.0198 |
| $10^{-2}$ | 237 | 1.15 | 1.25 | 99.1 | 0.109 | 0.0014 | 0.0110 |
| $\tau = 10$ | | | | | | | |
| 0 | 1.11 | 98.7 | 1.80 | 10.0 | 10.0 | 1.00 | 1.00 |
| $0^{-5}$ | 2.22 | 98.5 | 1.80 | 18.2 | 9.18 | 0.500 | 0.505 |
| $10^{-4}$ | 11.9 | 96.3 | 1.68 | 55.0 | 5.50 | 0.0908 | 0.100 |
| $10^{-3}$ | 72.3 | 75.7 | 1.44 | 91.8 | 1.82 | 0.0118 | 0.0198 |
| $10^{-2}$ | 128 | 53.3 | 1.34 | 99.1 | 1.09 | 0.0047 | 0.0110 |
| $\tau = 100$ | | | | | | | |
| 0 | 0.101 | 100 | 1.98 | - | - | 1.00 | 1.00 |
| $0^{-5}$ | 0.200 | 100 | 1.98 | - | - | 0.505 | 0.505 |
| $10^{-4}$ | 1.02 | 100 | 1.96 | - | - | 0.0990 | 0.100 |
| $10^{-3}$ | 5.37 | 99.5 | 1.89 | - | - | 0.0187 | 0.0198 |
| $10^{-2}$ | 10.0 | 98.8 | 1.82 | - | - | 0.0100 | 0.0110 |

(*Table 2 continued*)

JPET Fast Forward. Published on July 26, 2005 as DOI: 10.1124/jpet.105.090886
This article has not been copyedited and formatted. The final version may differ from this version.



[a] $EC_{50}$', $E_{max}$', $K_{obs}$' and $\tau_{obs}$' denote the corresponding parameter values of $EC_{50}$, $E_{max}$, $K_{obs}$ and $\tau_{obs}$ in the absence of allosteric modulator.

JPET Fast Forward. Published on July 26, 2005 as DOI: 10.1124/jpet.105.090886
This article has not been copyedited and formatted. The final version may differ from this version.



Table 3: Estimates of $EC_{50}$, $E_{max}$ and Hill slope for the simulated data in Figures 3*a* – *c*. In this example the allosteric modulator causes a ten-fold enhancement in both the affinity ($\alpha$ = 0.1) and intrinsic efficacy (ß = 10) of the agonist-receptor complex.

| *Allosteric Modulator (M)* | $EC_{50}$ *(μM)* | $E_{max}$ *(%)* | $K_{obs}$ *(μM)* | $\tau_{obs}$ | *Hill Slope* | $\frac{E_{max} EC_{50}'}{E_{max}' EC_{50}}$ [a] *(RA)* | $\frac{\tau_{obs} K_{obs}'}{\tau_{obs}' K_{obs}}$ [a] *(RA)* |
|---|---|---|---|---|---|---|---|
| *τ = 1* | | | | | | | |
| 0 | 5.00 | 50 | 10.0 | 1.00 | 1.0 | 1.00 | 1.00 |
| $10^{-6}$ | 0.847 | 84.6 | 5.50 | 5.50 | 1.0 | 9.98 | 10.0 |
| $10^{-5}$ | 0.179 | 90.2 | 1.82 | 9.18 | 1.0 | 50.4 | 50.5 |
| $10^{-4}$ | 0.0995 | 90.8 | 1.09 | 9.91 | 1.0 | 91.2 | 91.0 |
| $10^{-3}$ | 0.0918 | 90.9 | 1.01 | 9.99 | 1.0 | 98.9 | 99.0 |
| *τ = 10* | | | | | | | |
| 0 | 0.908 | 90.9 | 10.0 | 10.0 | 1.0 | 1.00 | 1.00 |
| $10^{-6}$ | 0.098 | 98.2 | 5.50 | 55.0 | 1.0 | 9.99 | 10.0 |
| $10^{-5}$ | 0.0196 | 98.9 | 1.82 | 91.8 | 1.0 | 50.3 | 50.5 |
| $10^{-4}$ | 0.0109 | 99.0 | 1.09 | 99.1 | 1.0 | 91.0 | 91.0 |
| $10^{-3}$ | 0.0100 | 99.0 | 1.01 | 99.9 | 1.0 | 99.1 | 99.0 |
| *τ = 100* | | | | | | | |
| 0 | 0.0990 | 99.0 | - | - | 1.0 | 1.00 | 1.00 |
| $10^{-6}$ | 0.0100 | 99.8 | - | - | 1.0 | 10.0 | 10.0 |
| $10^{-5}$ | 0.0020 | 99.9 | - | - | 1.0 | 50.6 | 50.5 |
| $10^{-4}$ | 0.0011 | 99.9 | - | - | 1.0 | 91.0 | 91.0 |
| $10^{-3}$ | 0.0010 | 99.9 | - | - | 1.0 | 99.1 | 99.0 |

(*Table 3 continued*)

JPET Fast Forward. Published on July 26, 2005 as DOI: 10.1124/jpet.105.090886
This article has not been copyedited and formatted. The final version may differ from this version.



[a] $EC_{50}$', $E_{max}$', $K_{obs}$' and $\tau_{obs}$' denote the corresponding parameter values of $EC_{50}$, $E_{max}$, $K_{obs}$ and $\tau_{obs}$ in the absence of allosteric modulator.

JPET Fast Forward. Published on July 26, 2005 as DOI: 10.1124/jpet.105.090886
This article has not been copyedited and formatted. The final version may differ from this version.



Table 4: Estimates of $EC_{50}$, $E_{max}$, Hill slope $K_{obs}$ and $\tau_{obs}$ for the simulated data in Figures 4*a – c*. In this example the allosteric modulator causes ten-fold increase in affinity ($\alpha$ = 0.1) and a ten-fold reduction in intrinsic efficacy ($ß$ = 0.1) of the agonist-receptor complex.

| *Allosteric Modulator (M)* | $EC_{50}$ *(μM)* | $E_{max}$ *(%)* | *Hill Slope* | $K_{obs}$ *(μM)* | $\tau_{obs}$ | $\frac{E_{max} EC_{50}' \, a}{E_{max}' EC_{50}}$ *(RA)* | $\frac{\tau_{obs} K_{obs}' \, a}{\tau_{obs}' K_{obs}}$ *(RA)* |
|---|---|---|---|---|---|---|---|
| *τ = 1* | | | | | | | |
| 0 | 5.00 | 50 | 1.0 | 10.0 | 1.00 | 1.00 | 1.00 |
| $10^{-6}$ | 3.55 | 35.5 | 1.0 | 5.50 | 0.550 | 1.00 | 1.00 |
| $10^{-5}$ | 1.54 | 15.4 | 1.0 | 1.82 | 0.182 | 1.00 | 1.00 |
| $10^{-4}$ | 0.98 | 9.82 | 1.0 | 1.09 | 0.109 | 1.00 | 1.00 |
| $10^{-3}$ | 0.92 | 9.17 | 1.0 | 1.01 | 0.101 | 1.00 | 1.00 |
| *τ = 10* | | | | | | | |
| 0 | 0.908 | 90.9 | 1.0 | 10.0 | 10.0 | 1.00 | 1.00 |
| $10^{-6}$ | 0.847 | 84.6 | 1.0 | 5.50 | 5.50 | 1.00 | 1.00 |
| $10^{-5}$ | 0.646 | 64.5 | 1.0 | 1.82 | 1.82 | 1.00 | 1.00 |
| $10^{-4}$ | 0.521 | 52.1 | 1.0 | 1.09 | 1.09 | 1.00 | 1.00 |
| $10^{-3}$ | 0.502 | 50.2 | 1.0 | 1.01 | 1.01 | 1.00 | 1.00 |
| *τ = 100* | | | | | | | |
| 0 | 0.0991 | 99.0 | 1.0 | - | - | 1.00 | 1.00 |
| $10^{-6}$ | 0.098 | 98.2 | 1.0 | - | - | 1.00 | 1.00 |
| $10^{-5}$ | 0.095 | 94.8 | 1.0 | - | - | 1.00 | 1.00 |
| $10^{-4}$ | 0.092 | 91.6 | 1.0 | - | - | 1.00 | 1.00 |
| $10^{-3}$ | 0.091 | 91.0 | 1.0 | - | - | 1.00 | 1.00 |

(*Table 4 continued*)

JPET Fast Forward. Published on July 26, 2005 as DOI: 10.1124/jpet.105.090886
This article has not been copyedited and formatted. The final version may differ from this version.



[a] $EC_{50}$', $E_{max}$', $K_{obs}$' and $\tau_{obs}$' denote the corresponding parameter values of $EC_{50}$, $E_{max}$, $K_{obs}$ and $\tau_{obs}$ in the absence of allosteric modulator.

JPET Fast Forward. Published on July 26, 2005 as DOI: 10.1124/jpet.105.090886
This article has not been copyedited and formatted. The final version may differ from this version.



Table 5: Estimates of $EC_{50}$, $E_{max}$, Hill slope and *RA* for the experimental data in Figure 9*a*.

| *Gallamine (M)* | $EC_{50}$[a] *(μM)* | $E_{max}$ *(% inhibition)* | *Hill Slope* | $\frac{E_{max} EC_{50}'}{E_{max}' EC_{50}}$[b] *(RA)* | $\frac{\tau_{obs} K_{obs}'}{\tau_{obs}' K_{obs}}$[b] *(RA)* |
|---|---|---|---|---|---|
| 0 | 1.26 (5.90 ± 0.16) | 54 ± 1.6 | 0.73 ± 0.11 | 1.0 | 1.0 |
| $10^{-6}$ | 3.54 (5.45 ± 0.091) | 49 ± 1.1 | 0.78 ± 0.007 | 0.32 (-0.50 ± 0.19) | 0.47 (-0.33 ± 0.11) |
| $3 \times 10^{-6}$ | 6.38 (5.20 ± 0.069) | 55 ± 1.0 | 0.95 ± 0.13 | 0.20 (-0.69 ± 0.14) | 0.17 (-0.77 ± 0.17) |
| $10^{-5}$ | 17.1 (4.77 ± 0.053) | 51 ± 3.2 | 0.96 ± 0.19 | 0.071 (-1.15 ± 0.18) | 0.079 (-1.10 ± 0.15) |
| $10^{-4}$ | 35.7 (4.45 ± 0.11) | 56 ± 1.9 | 0.95 ± 0.16 | 0.037 (-1.44 ± 0.11) | 0.029 (-1.54 ± 0.06) |
| $10^{-3}$ | 73.3 (4.14 ± 0.17) | 58 ± 3.2 | 0.63 ± 0.091 | 0.020 (-1.70 ± 0.37) | 0.018 (-1.76 ± 0.29) |

[a] The mean negative logarithm ± S.E.M. of each estimate of $EC_{50}$ is indicated in parentheses beneath each $EC_{50}$ estimate.

[b] The mean logarithm ± S.E.M. of each estimate of *RA* is indicated in parentheses beneath each *RA* estimate.

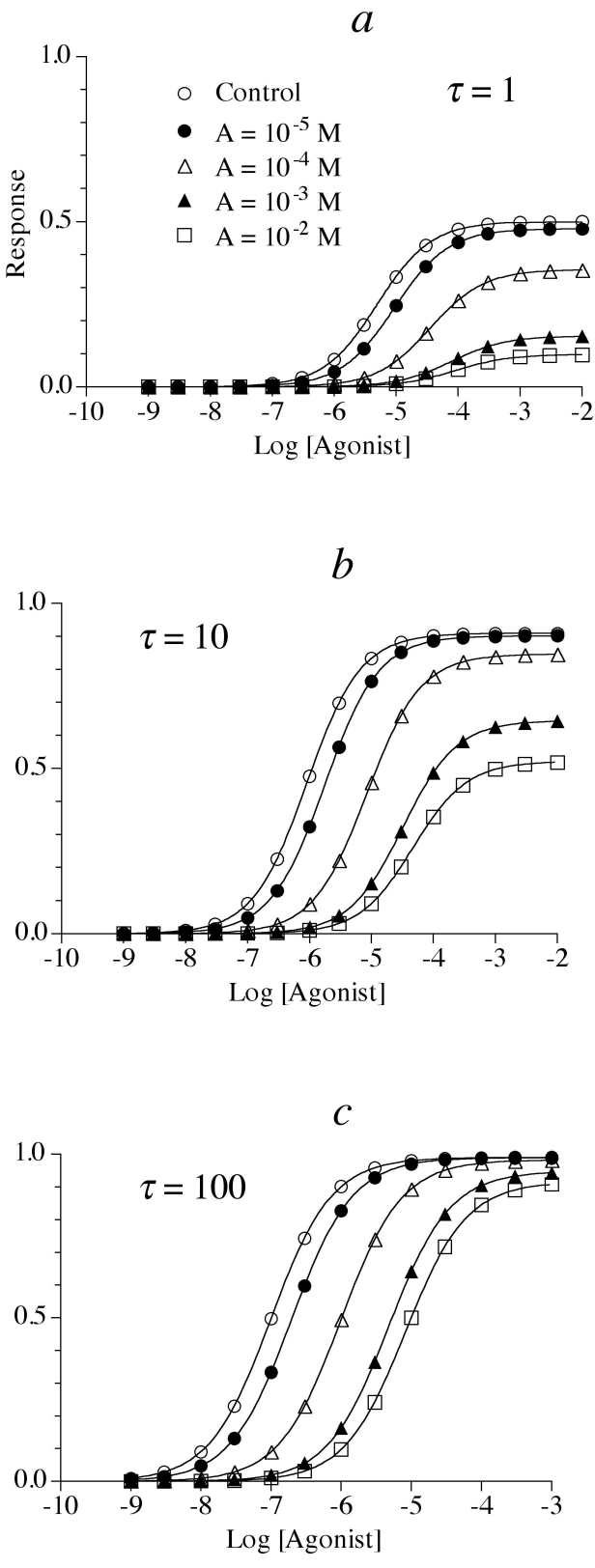
a
1.0
0.5
0.0
Response
Control
A = 10-5 M
A = 10-4 M
A = 10-3 M
A = 10-2 M
τ = 1
-10 -9 -8 -7 -6 -5 -4 -3 -2
Log [Agonist]
b
τ = 10
Log [Agonist]
c
τ = 100
Log [Agonist]

Figure 1

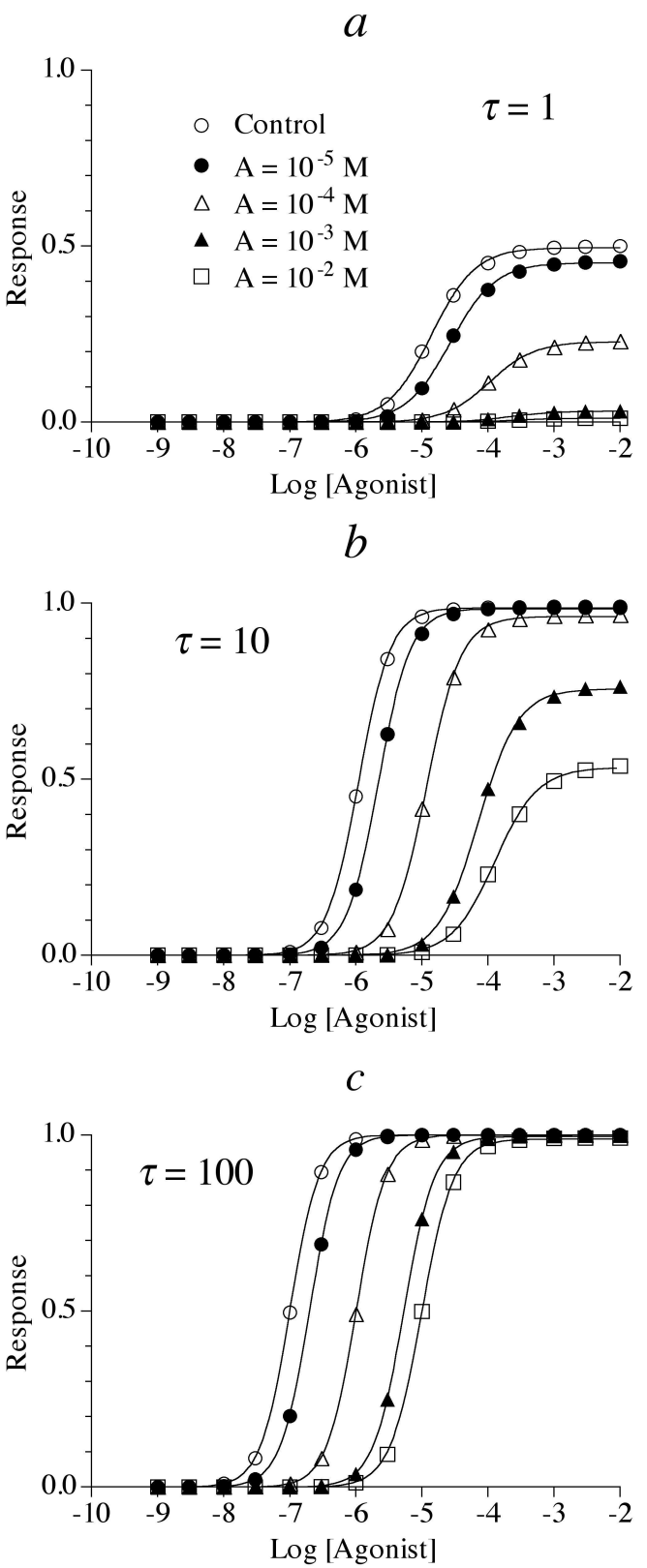
a
τ = 1
Control
A = 10-5 M
A = 10-4 M
A = 10-3 M
A = 10-2 M
Response
Log [Agonist]
b
τ = 10
Response
Log [Agonist]
c
τ = 100
Response
Log [Agonist]

Figure 2

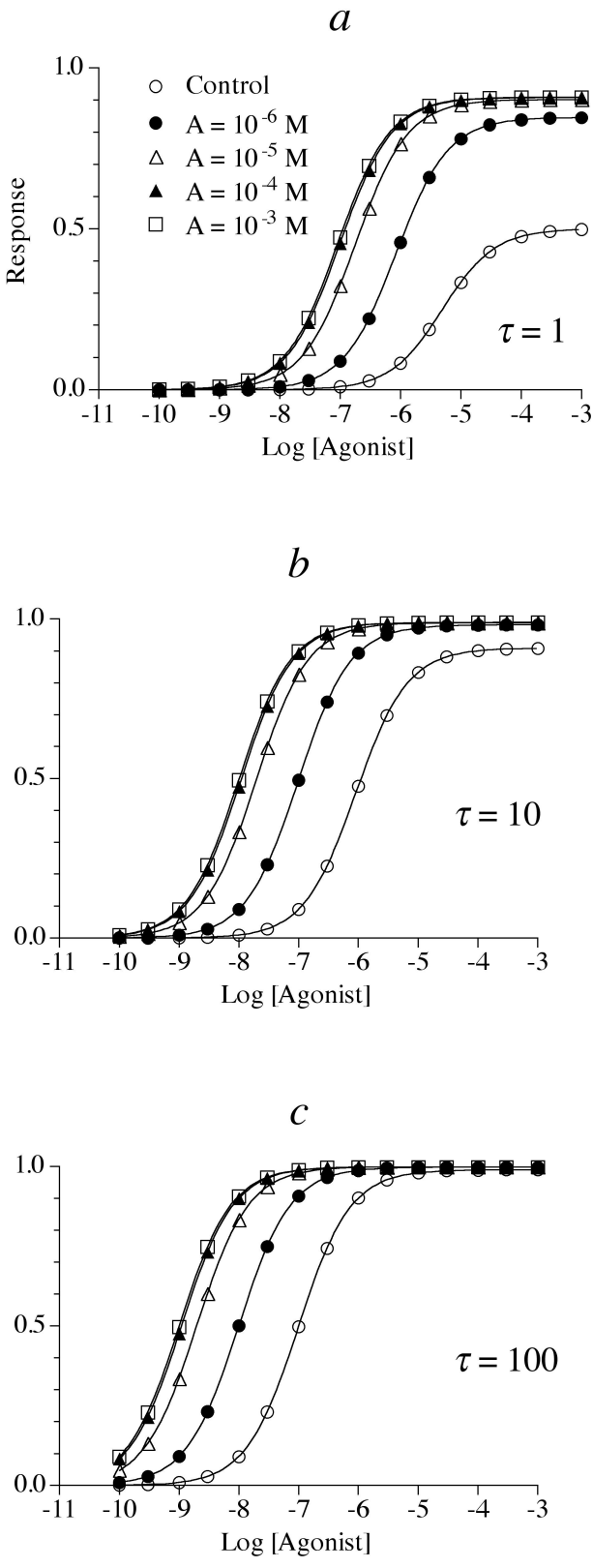
a
Control
A = 10-6 M
A = 10-5 M
A = 10-4 M
A = 10-3 M
τ = 1
Response
Log [Agonist]
b
τ = 10
Log [Agonist]
c
τ = 100
Log [Agonist]

Figure 3

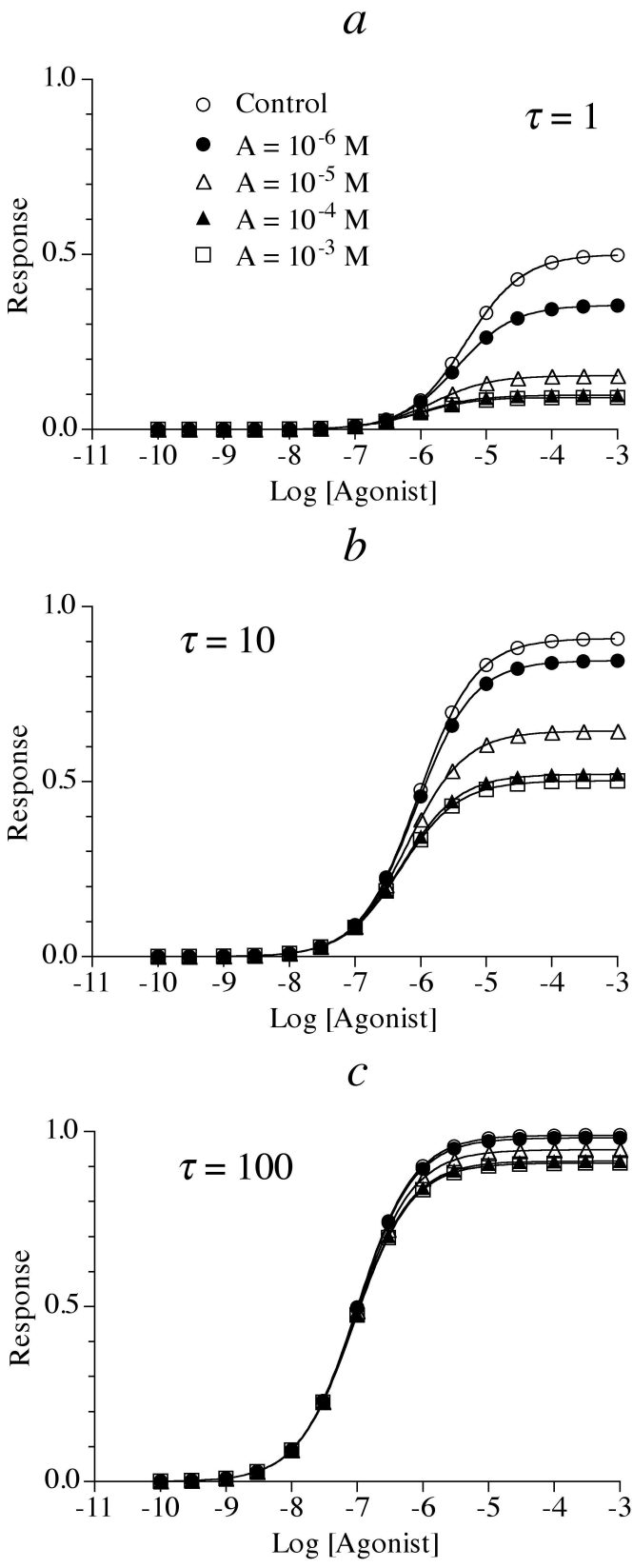
a
Control
A = 10-6 M
A = 10-5 M
A = 10-4 M
A = 10-3 M
τ = 1
Response
Log [Agonist]
b
τ = 10
Response
Log [Agonist]
c
τ = 100
Response
Log [Agonist]

Figure 4

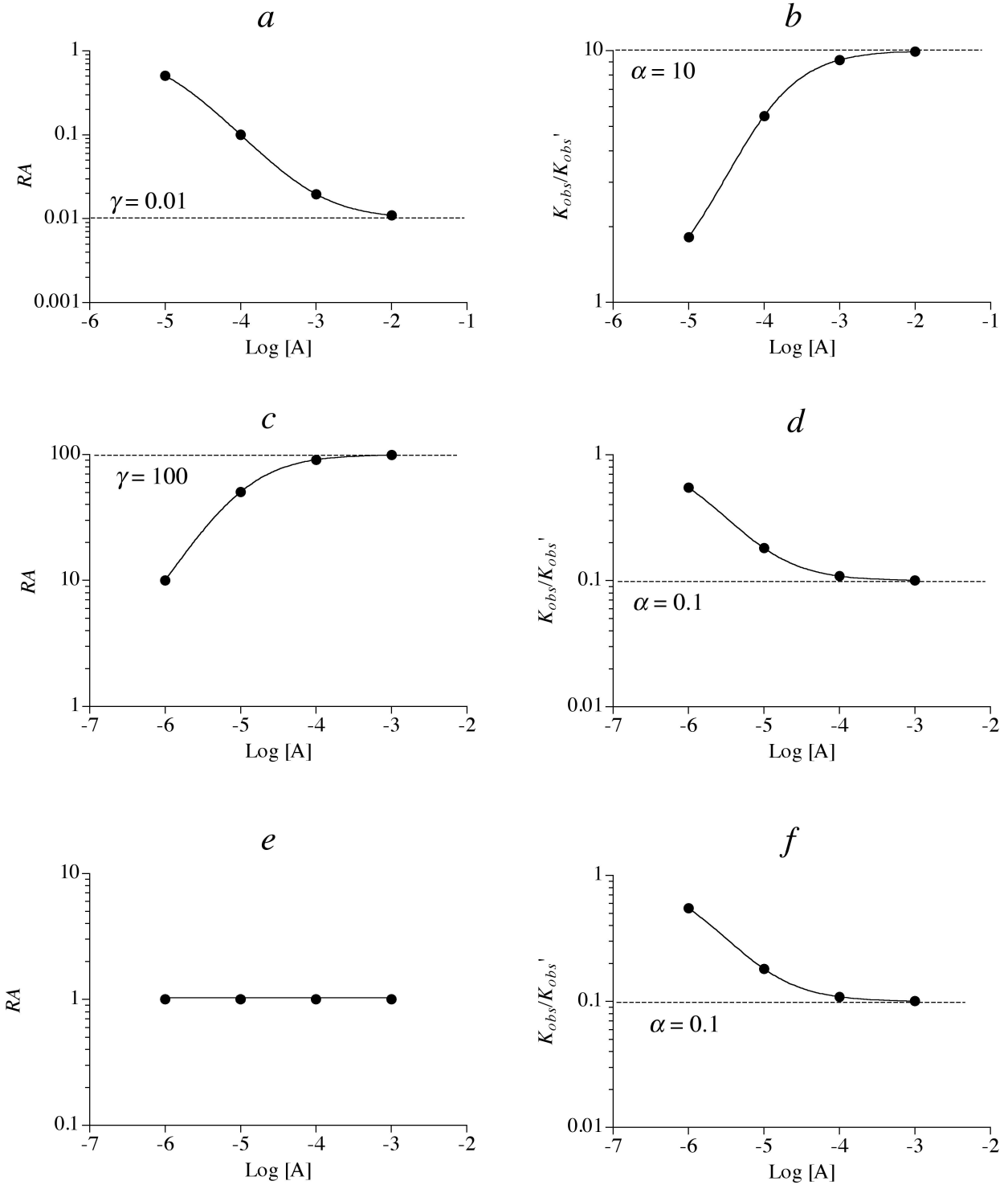
a
RA
γ = 0.01
Log [A]
b
α = 10
$K_{obs}/K_{obs}'$
Log [A]
c
RA
γ = 100
Log [A]
d
α = 0.1
$K_{obs}/K_{obs}'$
Log [A]
e
RA
Log [A]
f
α = 0.1
$K_{obs}/K_{obs}'$
Log [A]

Figure 5

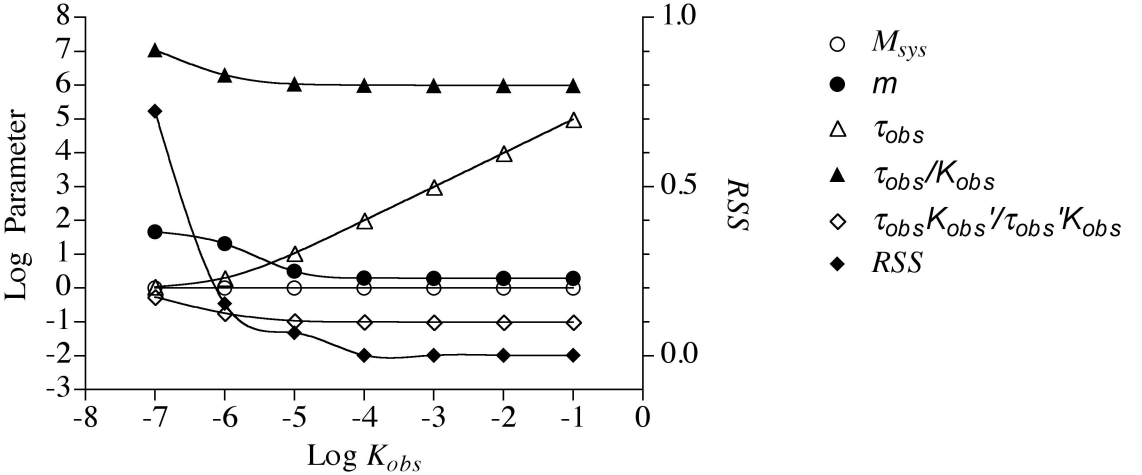
Log Parameter
Log $K_{obs}$
RSS
$M_{sys}$
$m$
$\tau_{obs}$
$\tau_{obs}/K_{obs}$
$\tau_{obs}K_{obs}'/\tau_{obs}'K_{obs}$
$RSS$

Figure 6

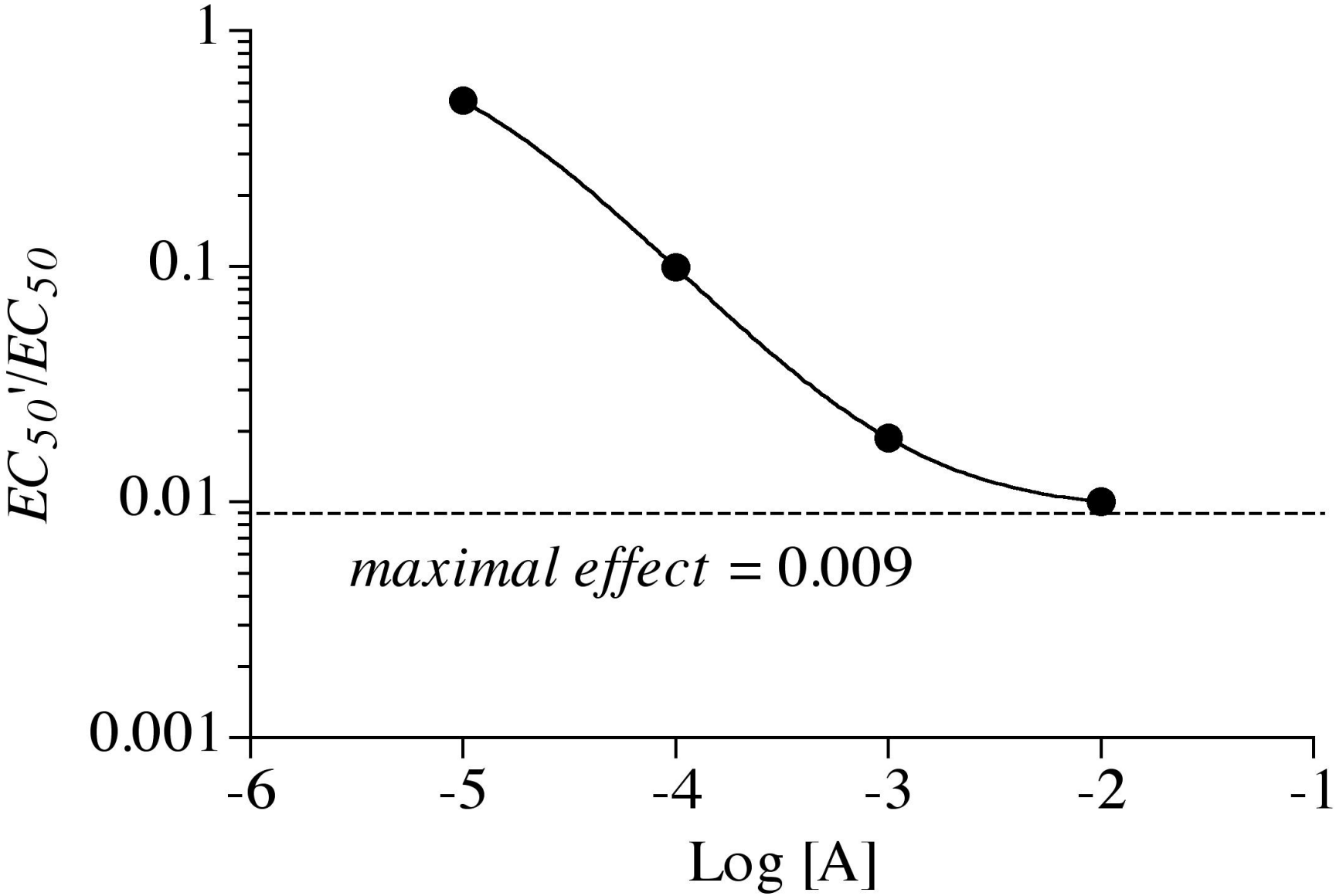


Figure 7

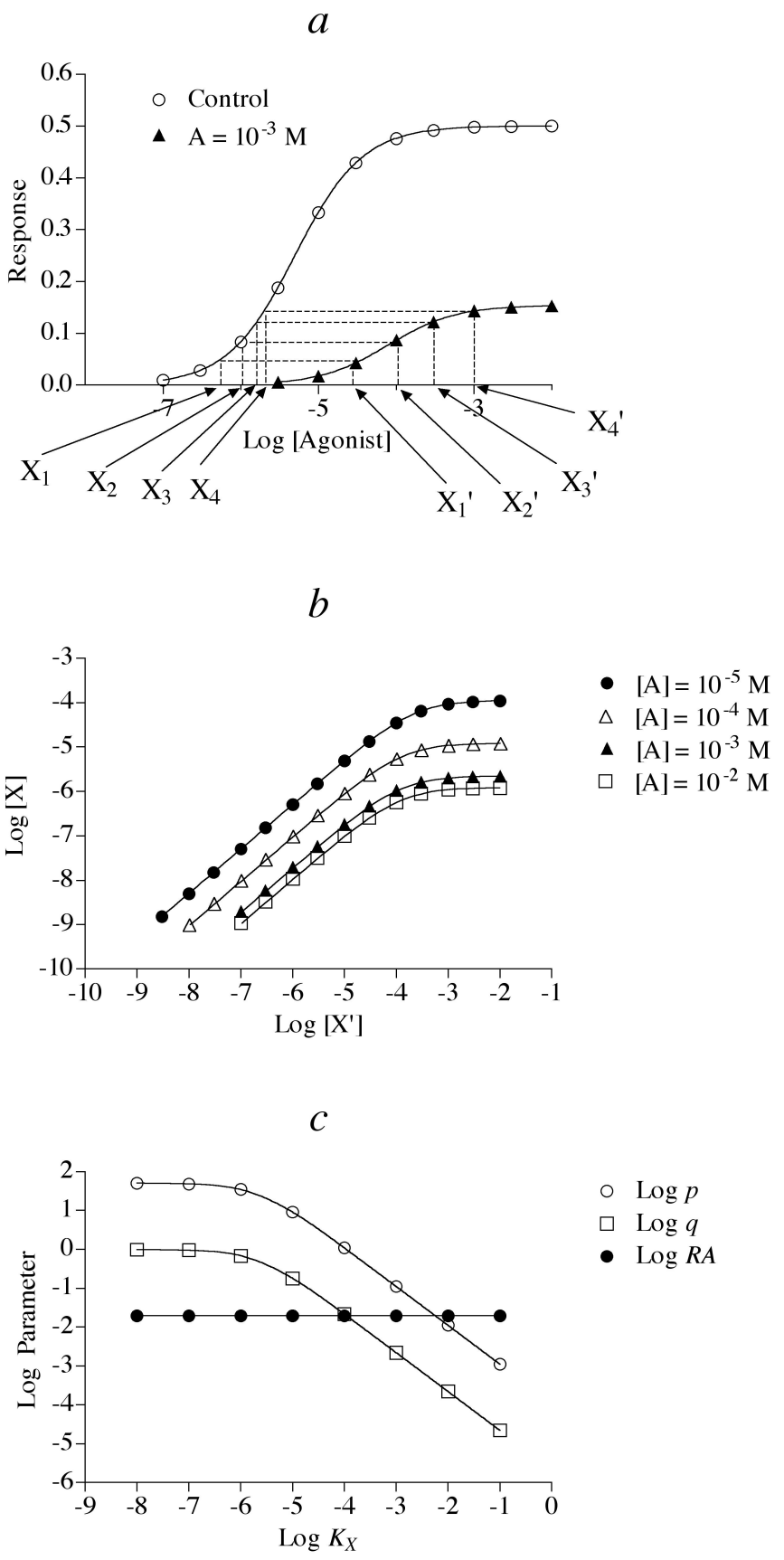
a
Control
A = 10-3 M
Response
Log [Agonist]
X1
X2
X3
X4
X1'
X2'
X3'
X4'
b
[A] = 10-5 M
[A] = 10-4 M
[A] = 10-3 M
[A] = 10-2 M
Log [X]
Log [X']
c
Log p
Log q
Log RA
Log Parameter
Log KX

**Figure 8**

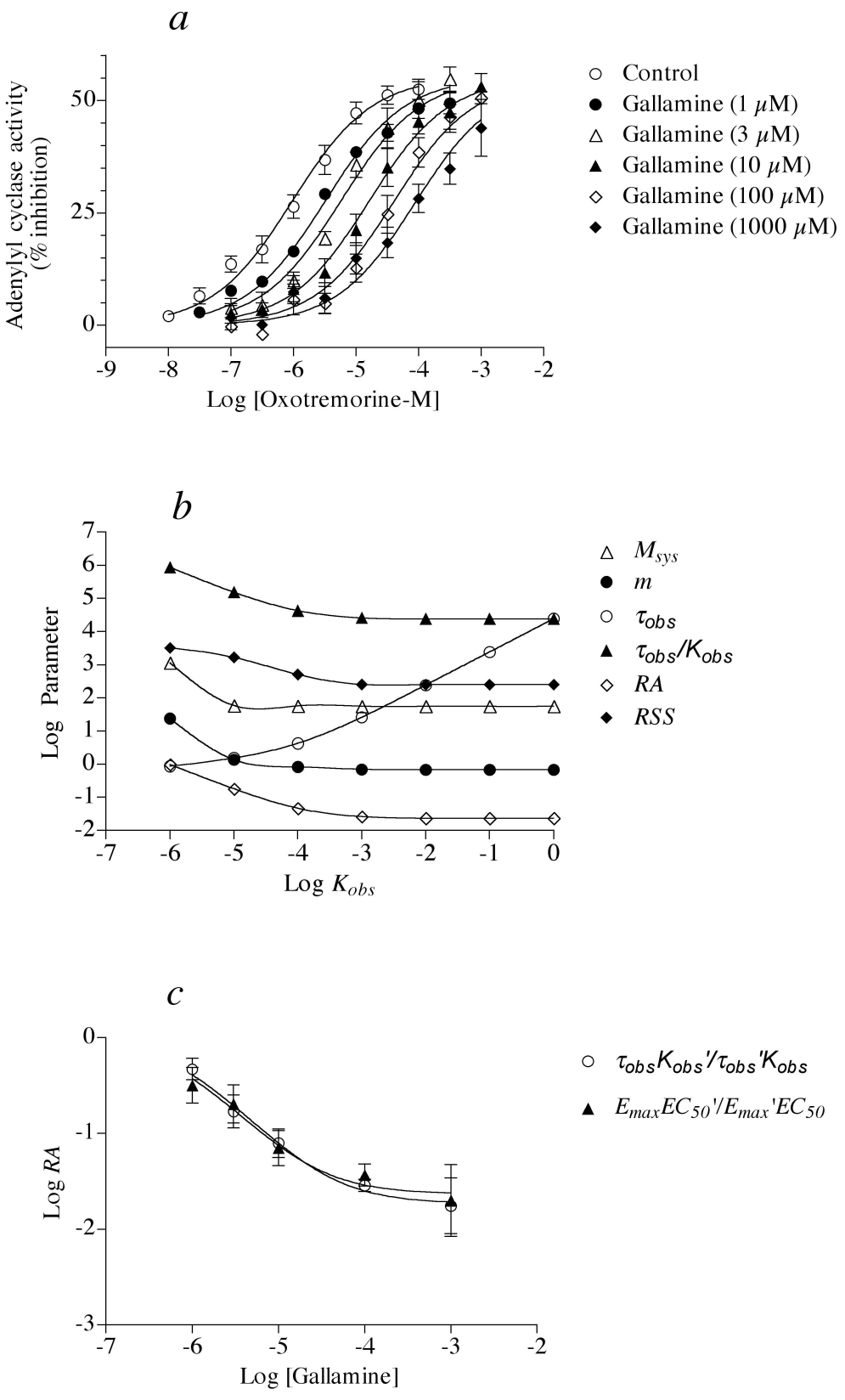
a
Adenylyl cyclase activity (% inhibition)
50
25
0
-9
-8
-7
-6
-5
-4
-3
-2
Log [Oxotremorine-M]
Control
Gallamine (1 μM)
Gallamine (3 μM)
Gallamine (10 μM)
Gallamine (100 μM)
Gallamine (1000 μM)
b
Log Parameter
7
6
5
4
3
2
1
0
-1
-2
-7
-6
-5
-4
-3
-2
-1
0
Log $K_{obs}$
$M_{sys}$
$m$
$\tau_{obs}$
$\tau_{obs}/K_{obs}$
$RA$
$RSS$
c
Log $RA$
0
-1
-2
-3
-7
-6
-5
-4
-3
-2
Log [Gallamine]
$\tau_{obs}K_{obs}'/\tau_{obs}'K_{obs}$
$E_{max}EC_{50}'/E_{max}'EC_{50}$

Figure 9